Metis Coronagraph
Ground Calibration

Silvano Fineschi

INAF – Osservatorio Astrofisico di Torino, Italy

On behalf of the Metis Team

VI Metis Workshop – Gottingen, D, 21 November 2018

OAC OACt OATs

Outline

- Solar Orbiter/Metis
  - General introduction
  - Instrument description
- Calibration facility and setup
- Instrument Calibrations
  - **Vignetting function (Flat-Field)**
  - **VLDA Photon Transfer Curve**
  - **VL & UV Imaging & Radiometric Performance**
  - **VL Polarimeter Performance**
  - **Stray-light Suppression Performance and internal occulter centering**
- Conclusions

In short

It works!

OAC OACt OATs

Metis Coronagraph

- Polarized VL imaging @ 580 - 640 nm
- UV HI Ly α imaging @ 121.6 ± 10 nm
- FoV (1.5° · 2.9° annular, 1.6 – 3.0 $R_{\odot}$ @ 0.28 AU)
- Spatial sampling element ≤ 4000 km (20”) @ 0.28 AU
- Time resolution ≥ 1 sec
- Simultaneous VL and UV imaging

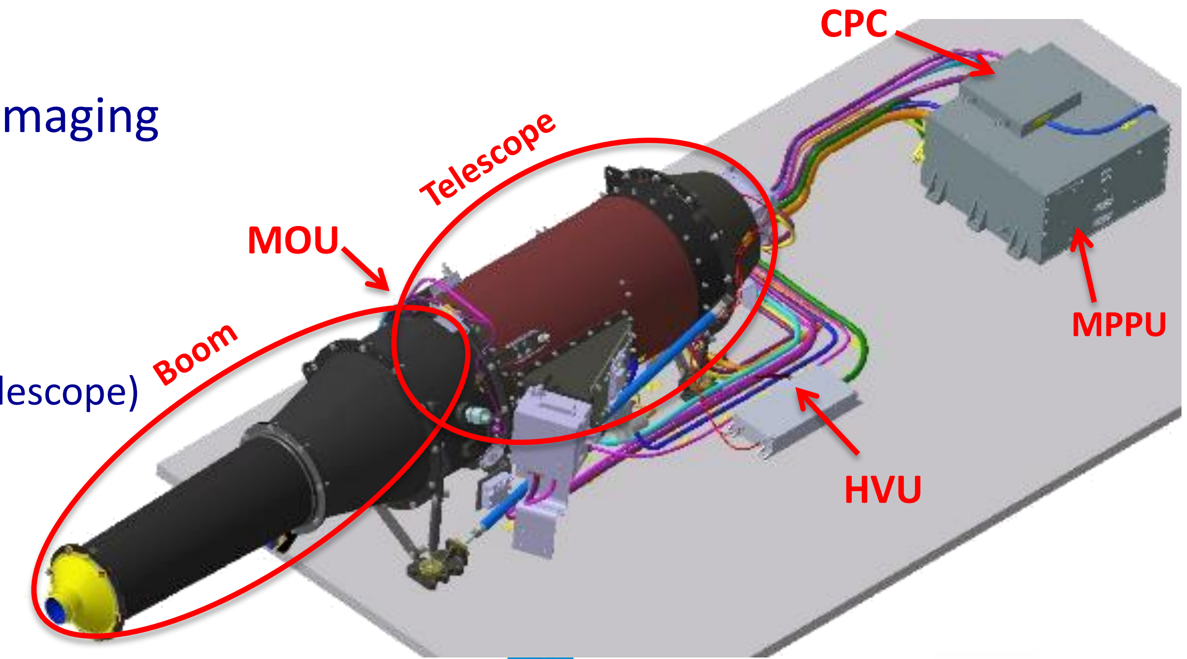

Units:
MOU METIS Optical Unit (boom and telescope)
MPPU METIS Power Processing Unit
HVU High Voltage Unit
CPC Camera Power Converter

Metis Opto-mech Layout

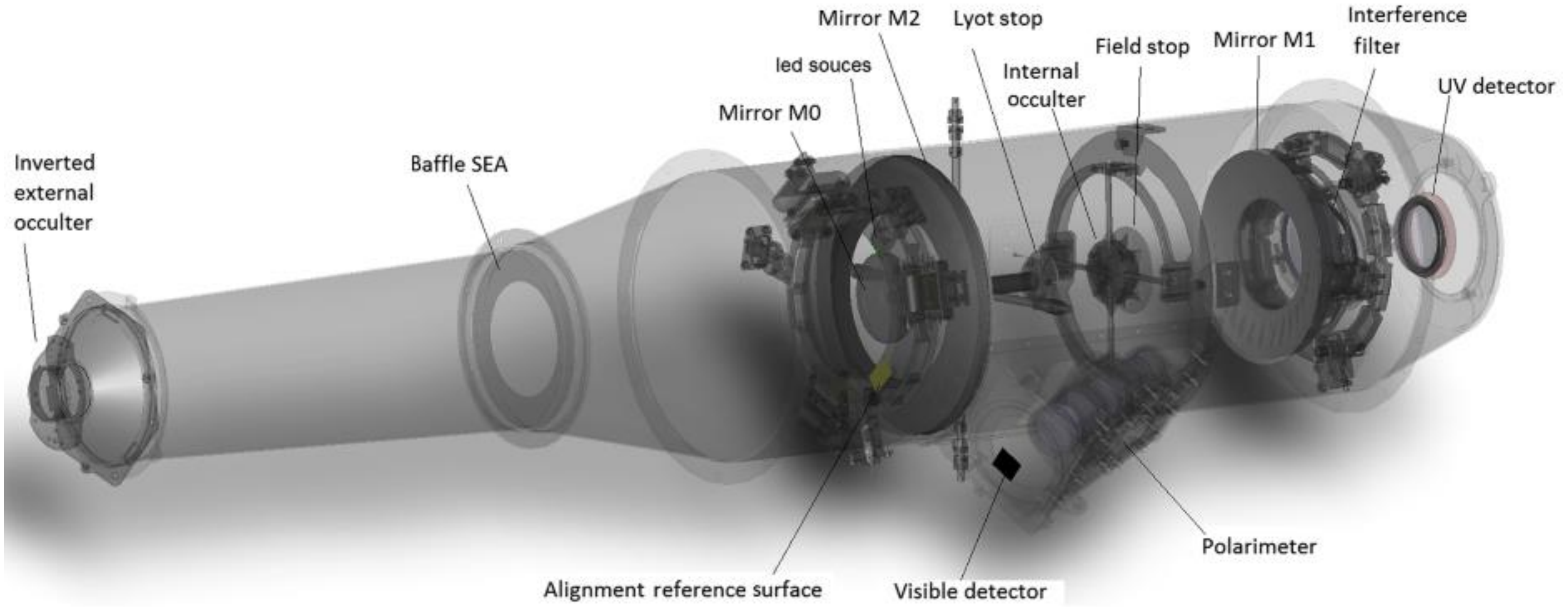

Ground Calibration Facility

- AIT/AIV and calibrations were performed at the OPSys (Optical Payload System) facility, an INAF laboratory hosted by ALTEC S.p.A. in Torino.
- OPSys: three communicating clean rooms which host the SPOCC (Space Optics Calibration Chamber)

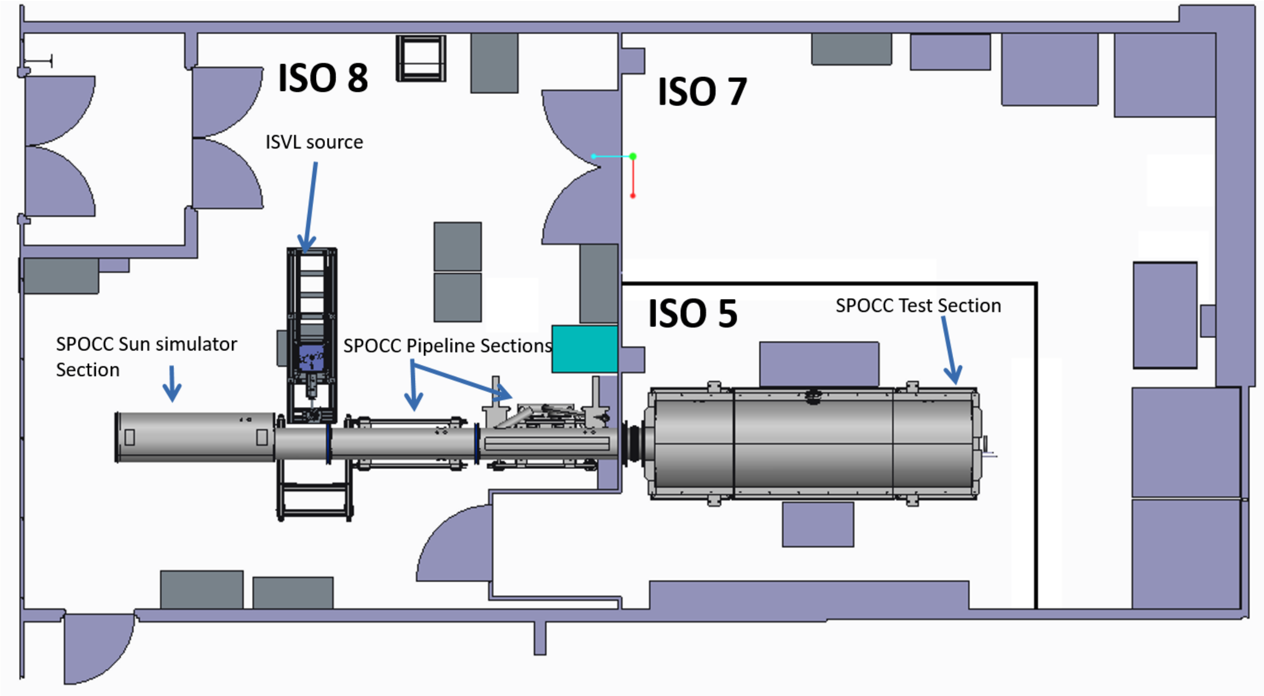

- SPOCC is a solar divergence simulator that can operate in air and in vacuum.

Metis in the
Space Optics Calibration Chamber (SPOCC)

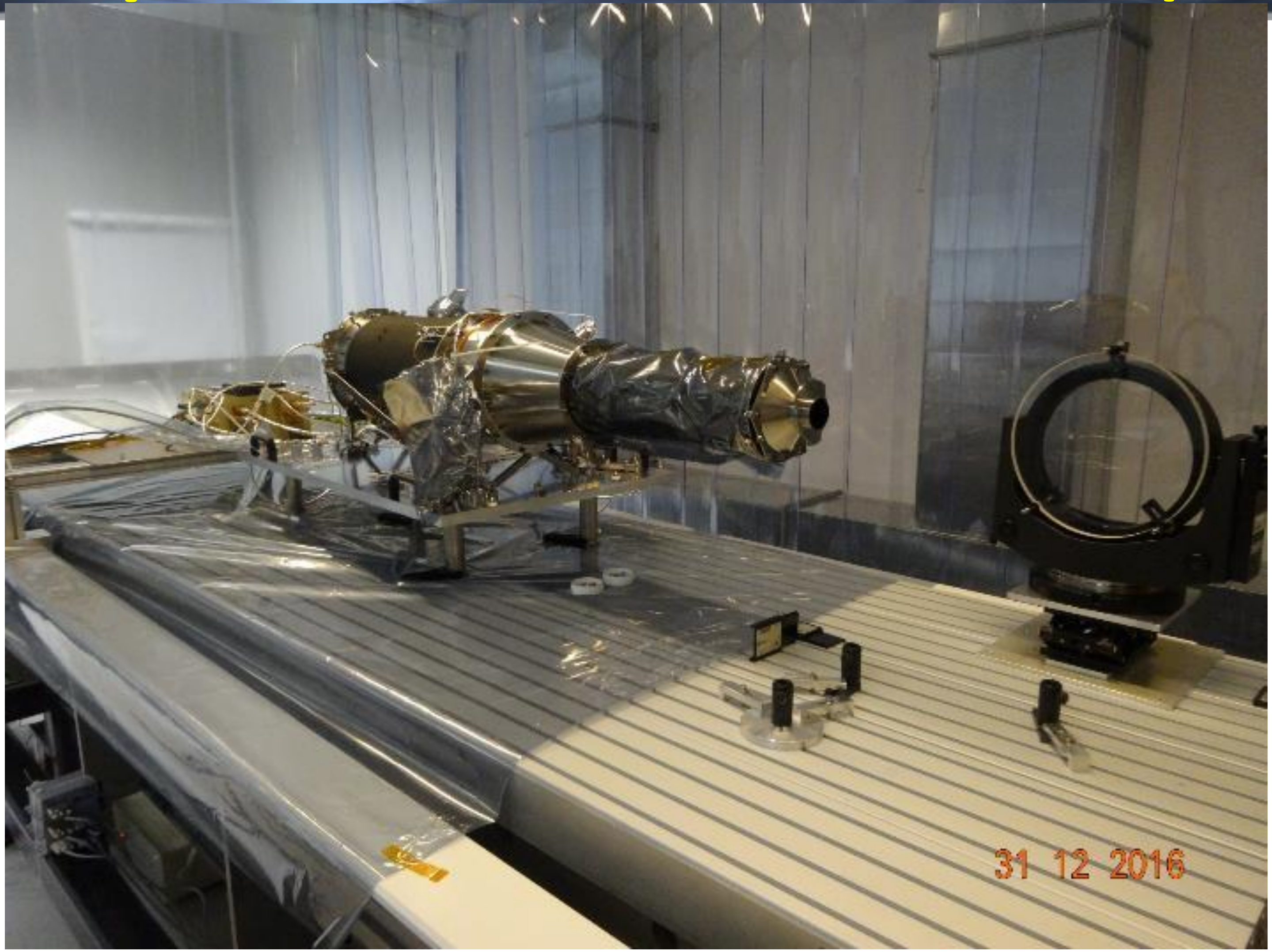

IFN ASF ifsi OAC OACt CAIfA OATs OHB CGS ThalesAlenia Space

Metis in the Space Optics Calibration Chamber (SPOCC)

Ground Calibrations

- Vignetting function (VL Flat-Field)
- VLDA Photon Transfer Curve
- VL & UV Imaging & Radiometric Performance
- VL Polarimeter Performance
- Stray-light Suppression Performance
- Internal occulter centering

OAC OACt OATs

Vignetting Function & VL Flat Field

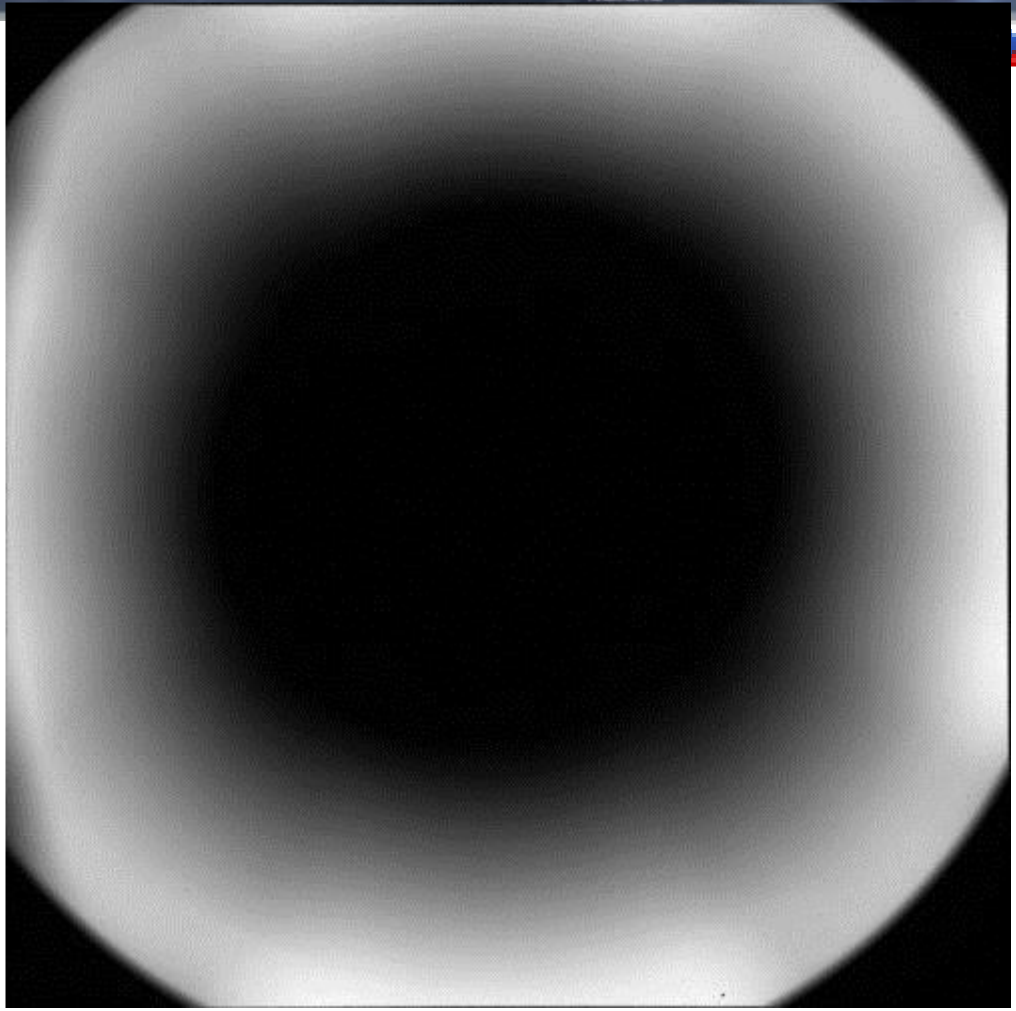

Vignetting Function & Flat Field

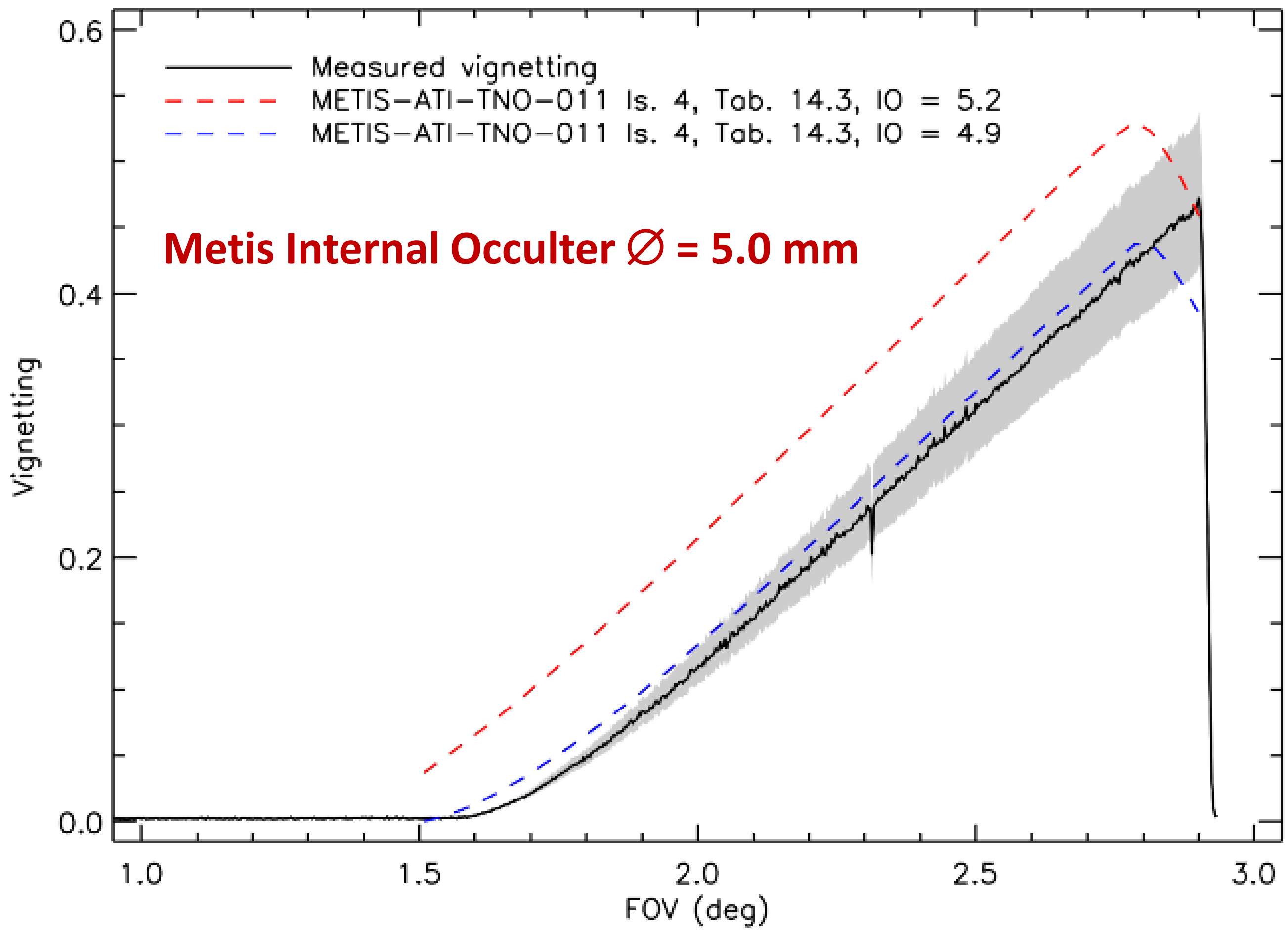

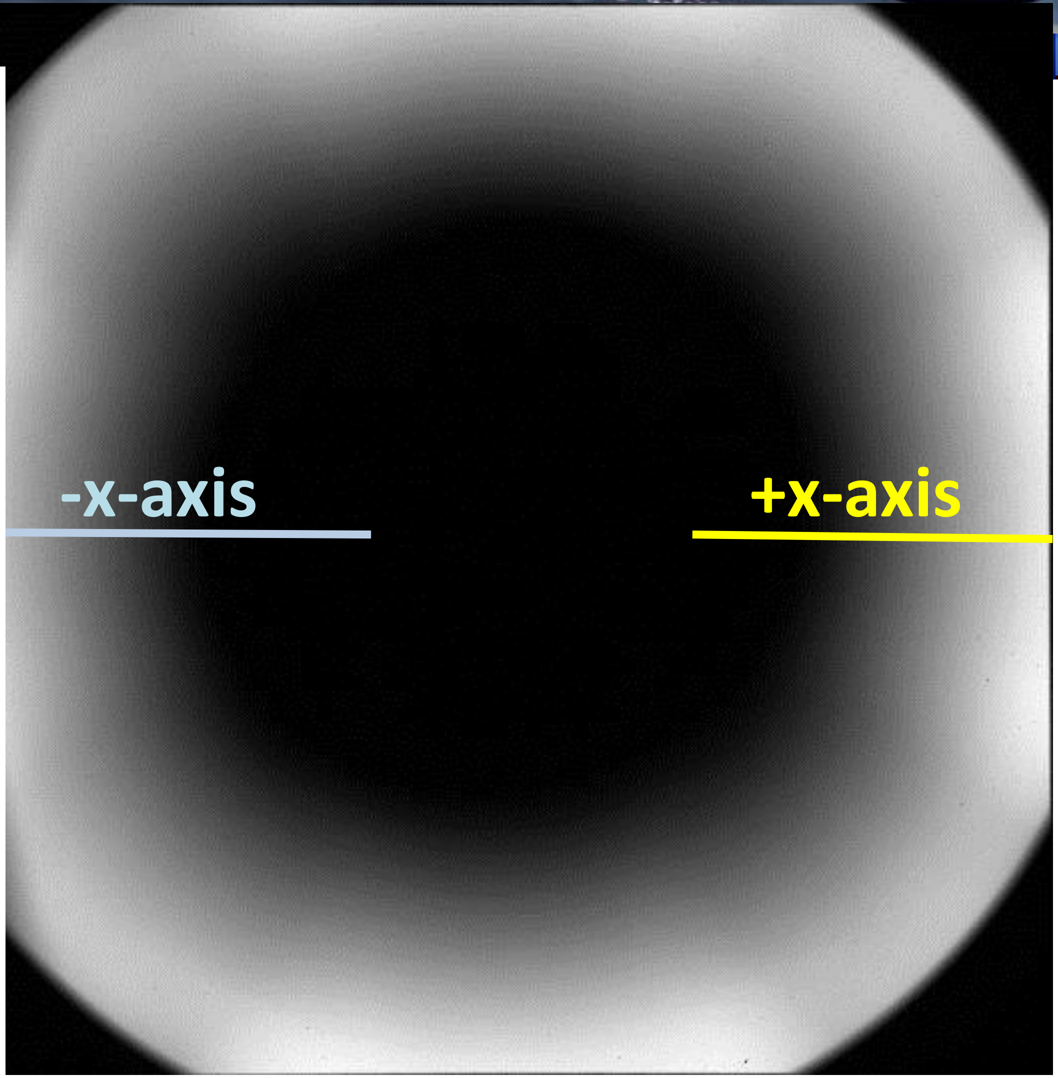

VLDA Photon Transfer Curve

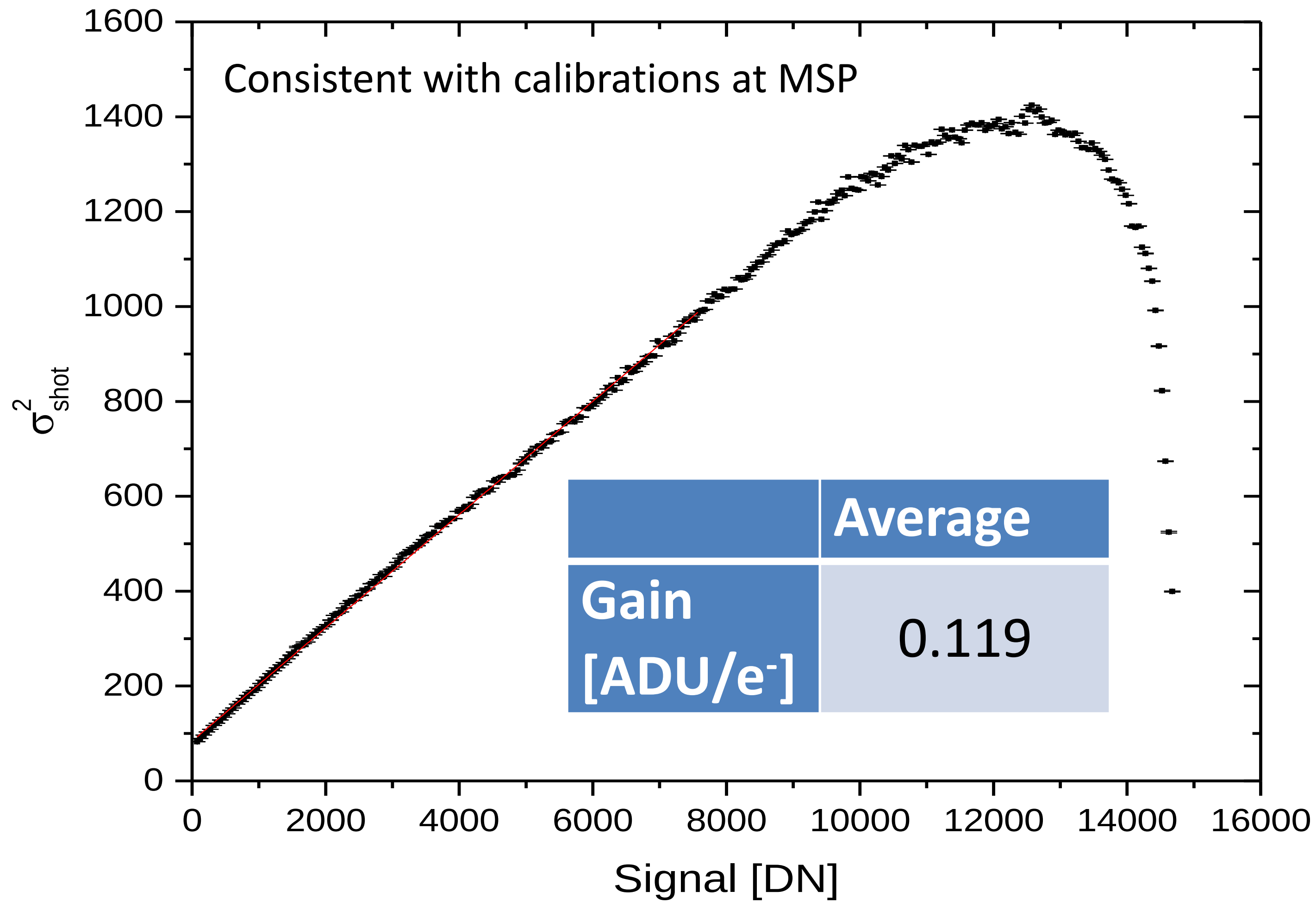

	Average
Gain [ADU/e$^-$]	0.119

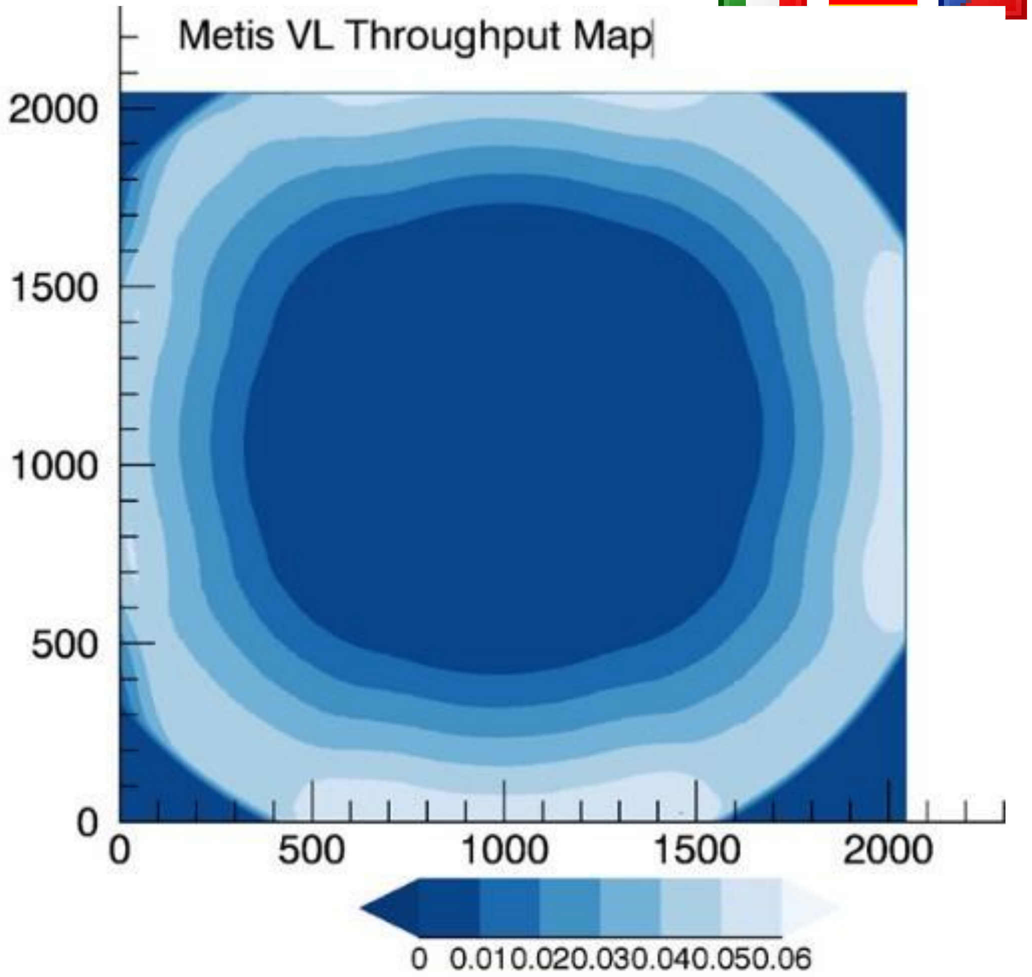

VL Measured Efficiency

Visible-light			
Component	**Efficiency**	**Error**	**Reference**
M1	0.9	0.02	METIS-ANT-NCR-018 Appendix 1 INF 28/07/2016
M2	0.9	0.02	
IFA	0.886	0.001	INAF Fineschi et al. 22/092016
Polarimeter	0.33	0.05	METIS- ATI-TNO-011 (estim.: 0.27) 0.33 Measued on the EBB with Muller SpectroPolarimeter
QE	0.5	0.05	METIS-MPS-AT-03b-PFM-RP0005 Issue 1 rev 1. Sect 6.10, Figure 6.29
Total efficiency	0.118	0.012	
Estim. Tot. Eff.	0.096		METIS- ATI-TNO-011 (Tab.14-1)

VL Vignetting Normalization

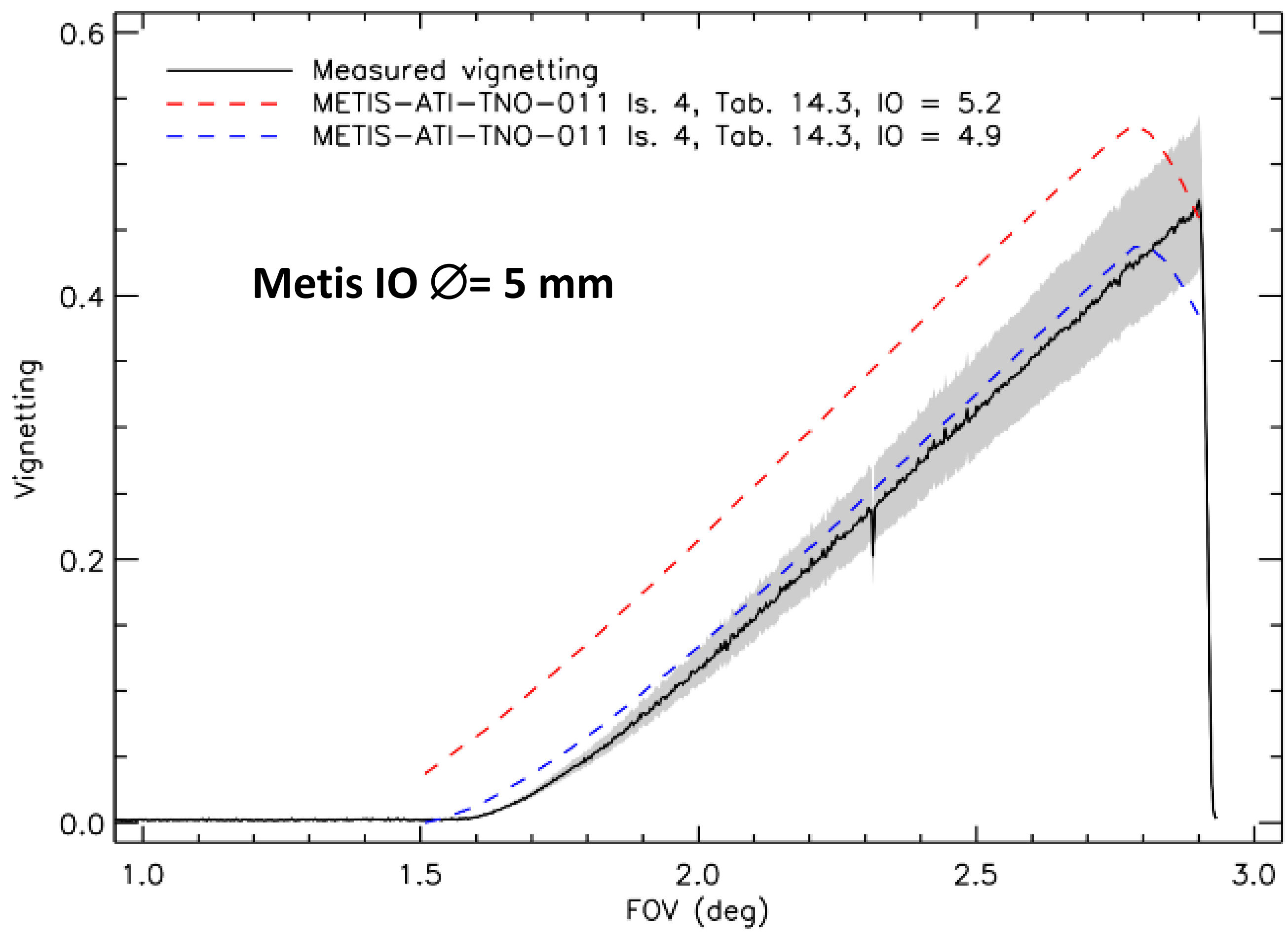

Vignetting =

= Meas. Throughput [phot. detect./phot. in] / Efficiency

(Efficiency = 0.10±0.01 from components measurements)

Off-axis Metis in SPOCC

Metis set-up for VL and UV Measurements

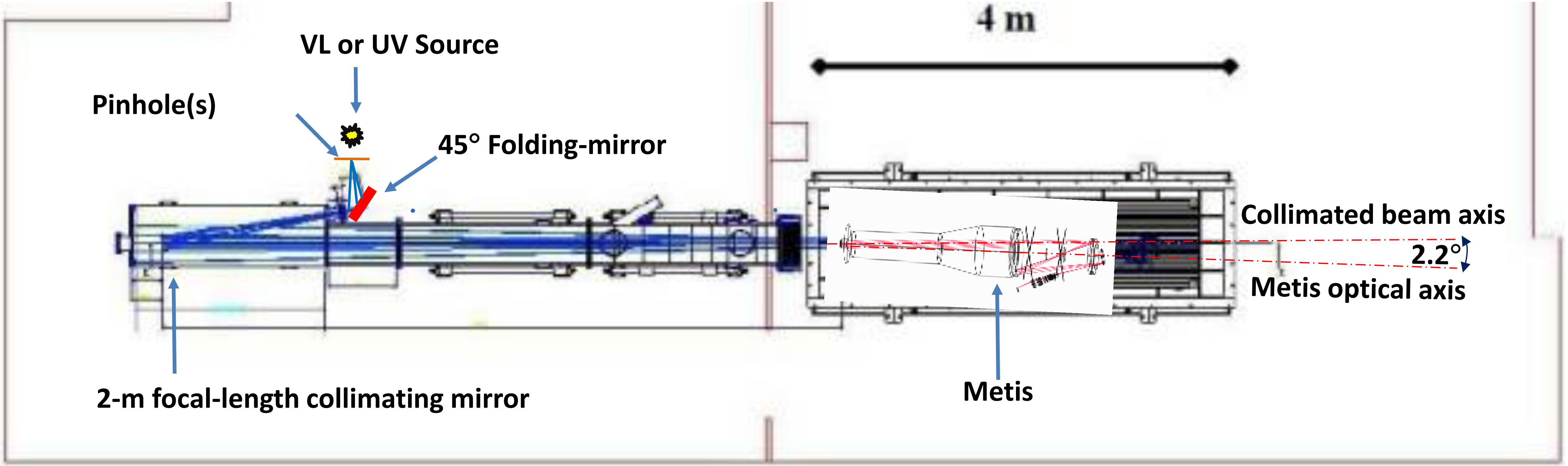

VL Imaging Performance

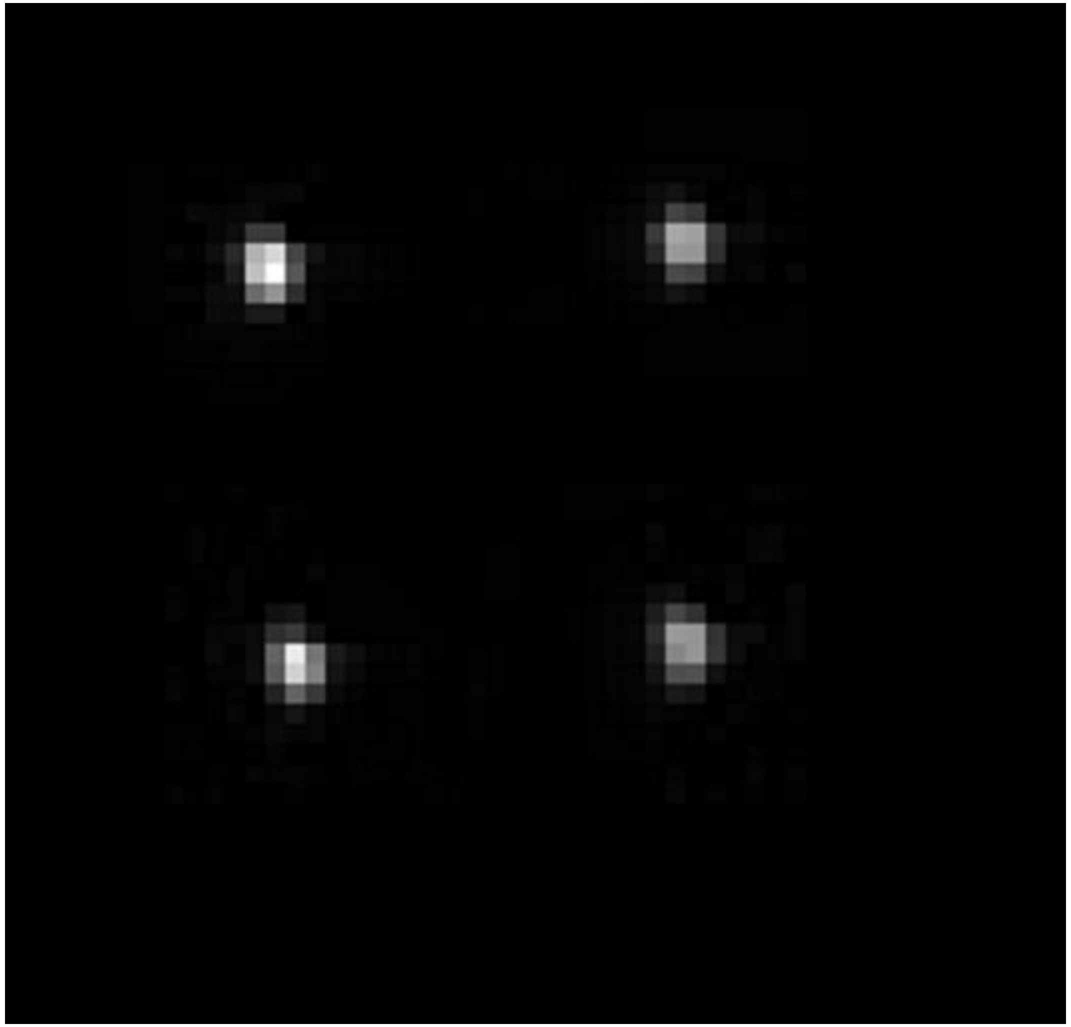

Target:
200-μm pinhole $\times$ 4
SPOCC collimator f.l. = 2030 mm
VL effective f.l. = 200 mm
Demagnification = 0.098

simulating 4 “artificial stars”
with 20-μm FWHM on VLDA

VL Imaging Performance vs Field-of-View

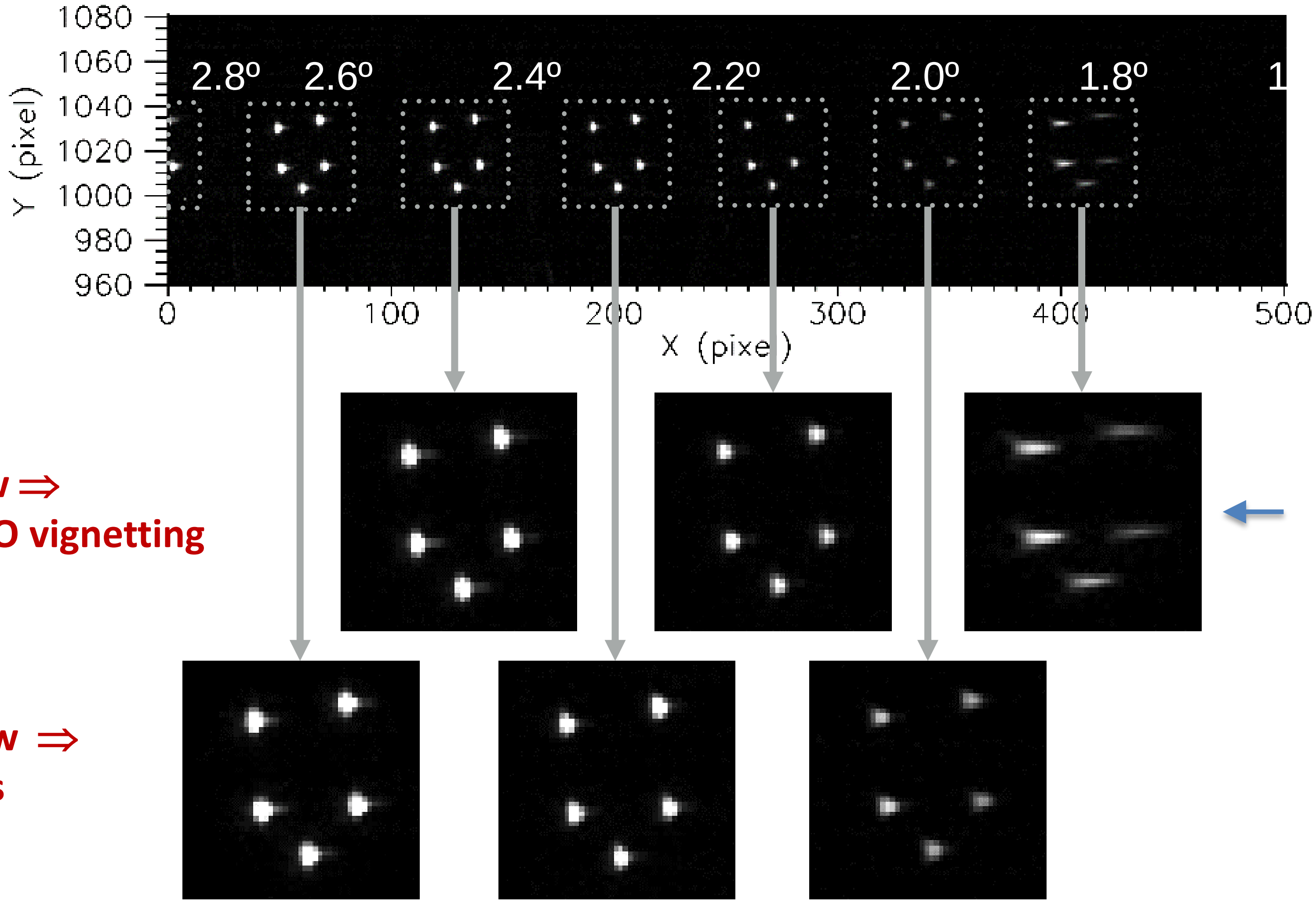

- **Inner Field-of-View ⇒ Diffraction from IEO vignetting**
- **Outer Field-of-View ⇒ Optical aberrations**

Natural diffraction due to the highly vignetted inner FOV

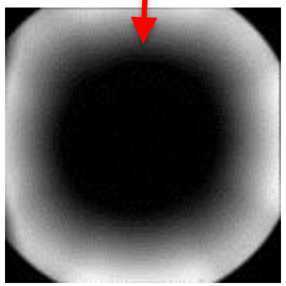

VL Imaging Performance vs Field-of-View

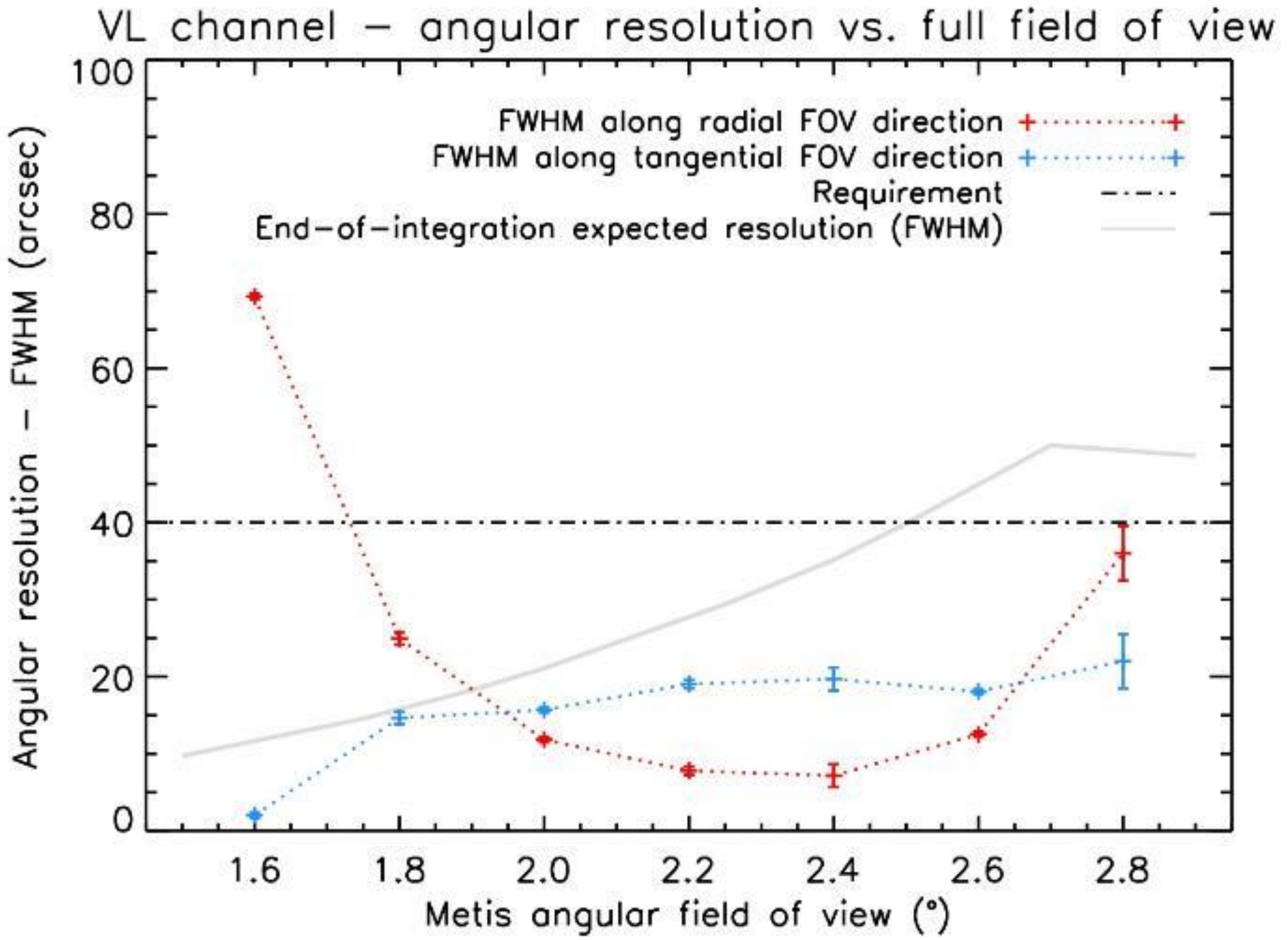

VL Imaging Performance

⇓

well within requirements

VL Radiometric Response

Metis off-pointed at 2.2° sees an “artificial Sun” at 1 AU

VL Radiometric Response =

VLDA signal (DN/s/pxl)/Input Radiance (W/cm²/sr)

VL Throughput @ FOV 2.2° =

= (1.9 ± 0.2) e-2

(estimate based on component-level: 2.3 e-2)

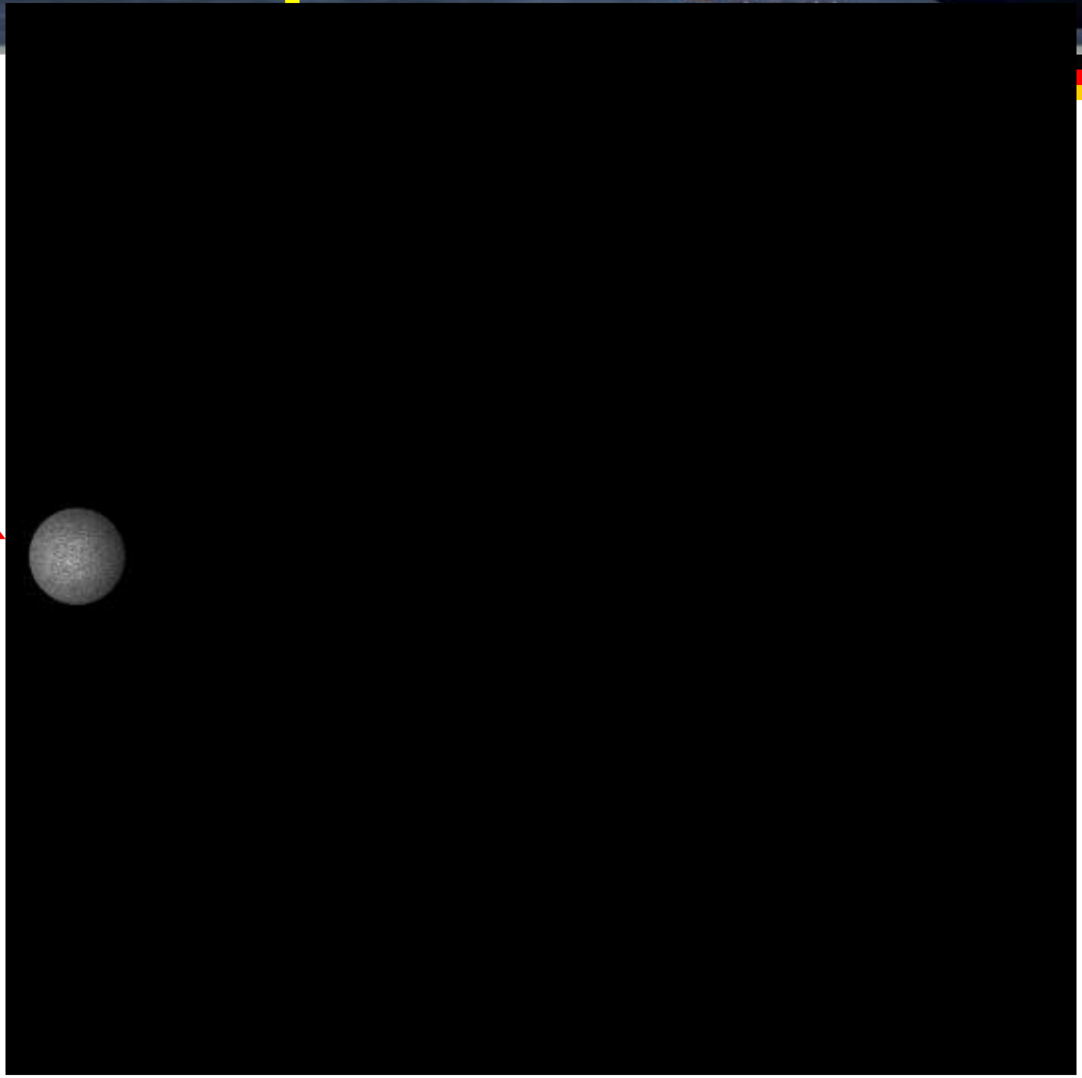

UV-analog Imaging Performance vs FoV

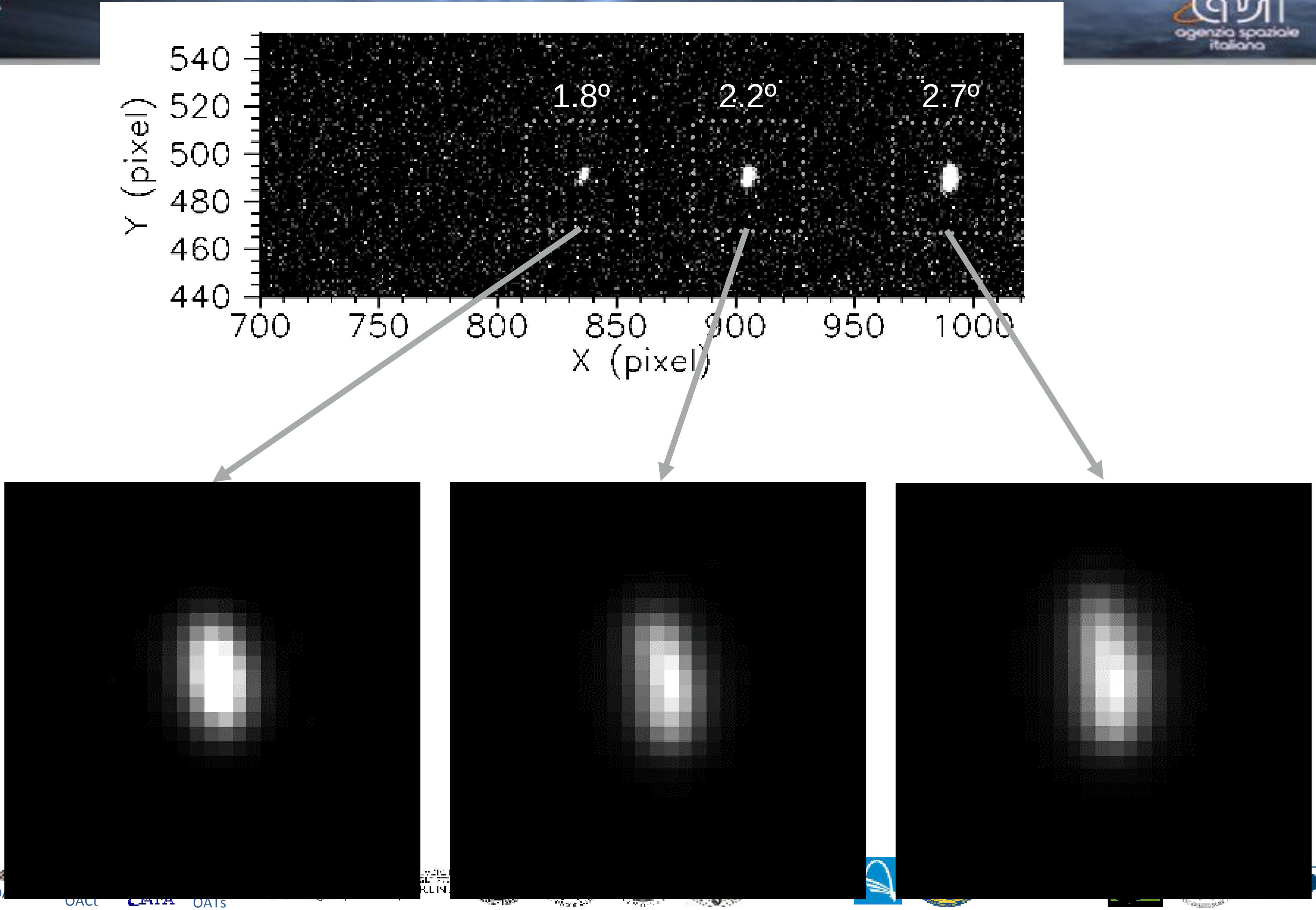

UV-analog Imaging Performance vs FoV

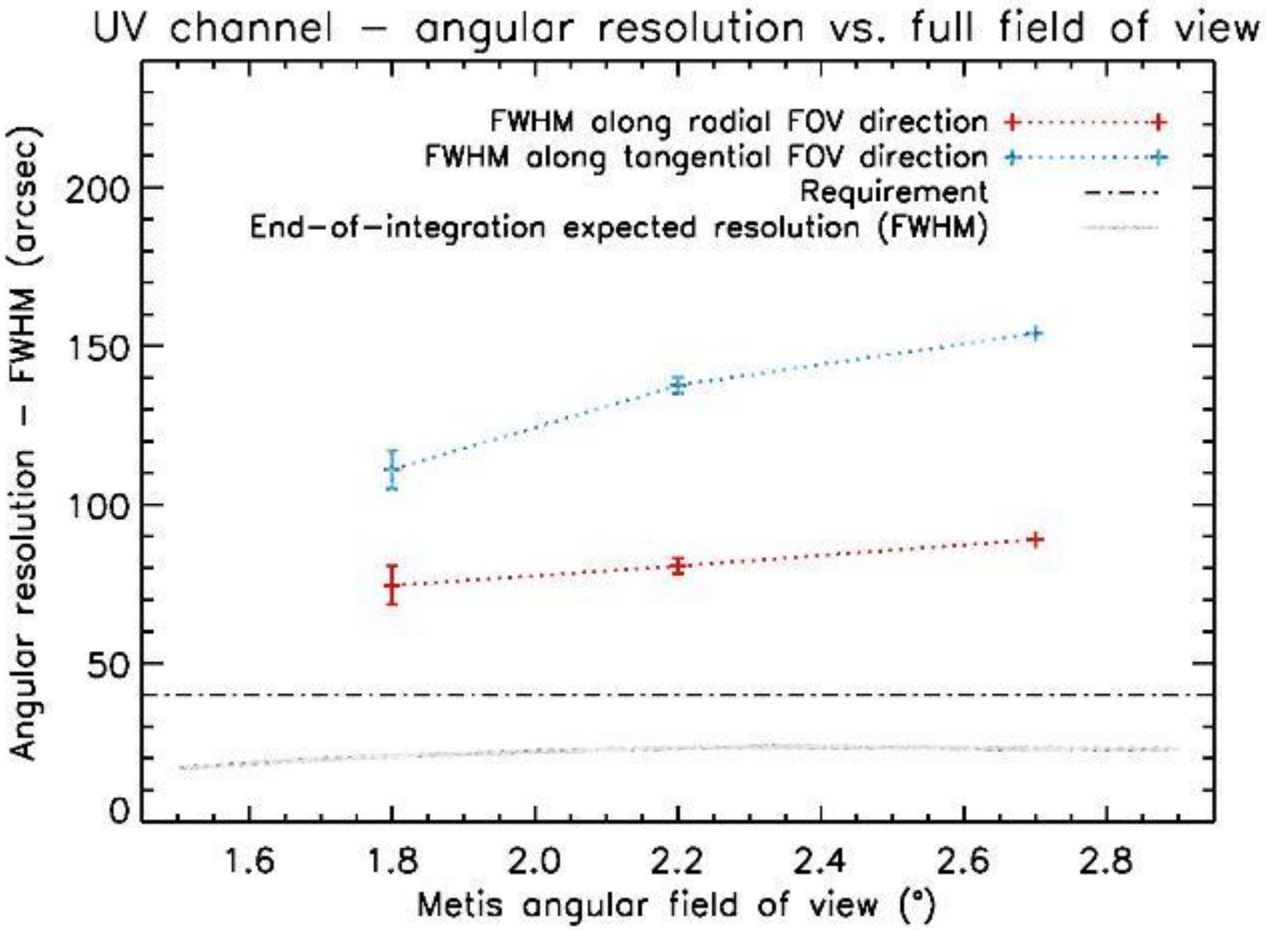

The UV imaging performances, when the UVDA is operated in analog mode, are limited in spatial resolution to: 3-4 pixel ⇒ 80-100 arcsec

Cfr.

P62 F. Frassetto: Optical performance

P71 V. Da Deppo: Alignment procedure

UV Throughput Estimated from Components Measurements

UV (121.6 nm)			
Component	**Efficiency**	**Error**	**Reference**
M1	0.54	0.12	Bear 02/10/2016 (T=0.77) &
M2	0.54	0.12	IFN 29/09/2016 (T=0.77); IFN 09/09/2017 (T=0.59); IFN 10/01/2017 (T=0.54)
IFA	0.24	0.04	INAF Fineschi et al. note 22/092016 Selected FM=0.24 (email by E. Antonucci Tue, 27 Sep 2016)
MgF2 window	0.18		MPS private communication
QE			
Total efficiency	0.013	0.004	
Efficiency w/o QE	0.07	0.02	0.36
Estim. Eff. w/o QE	0.16		
Eff. Estim./Meas.	2.27		

UV Throughput

E2E Measurements vs Estimated from Components Measurements

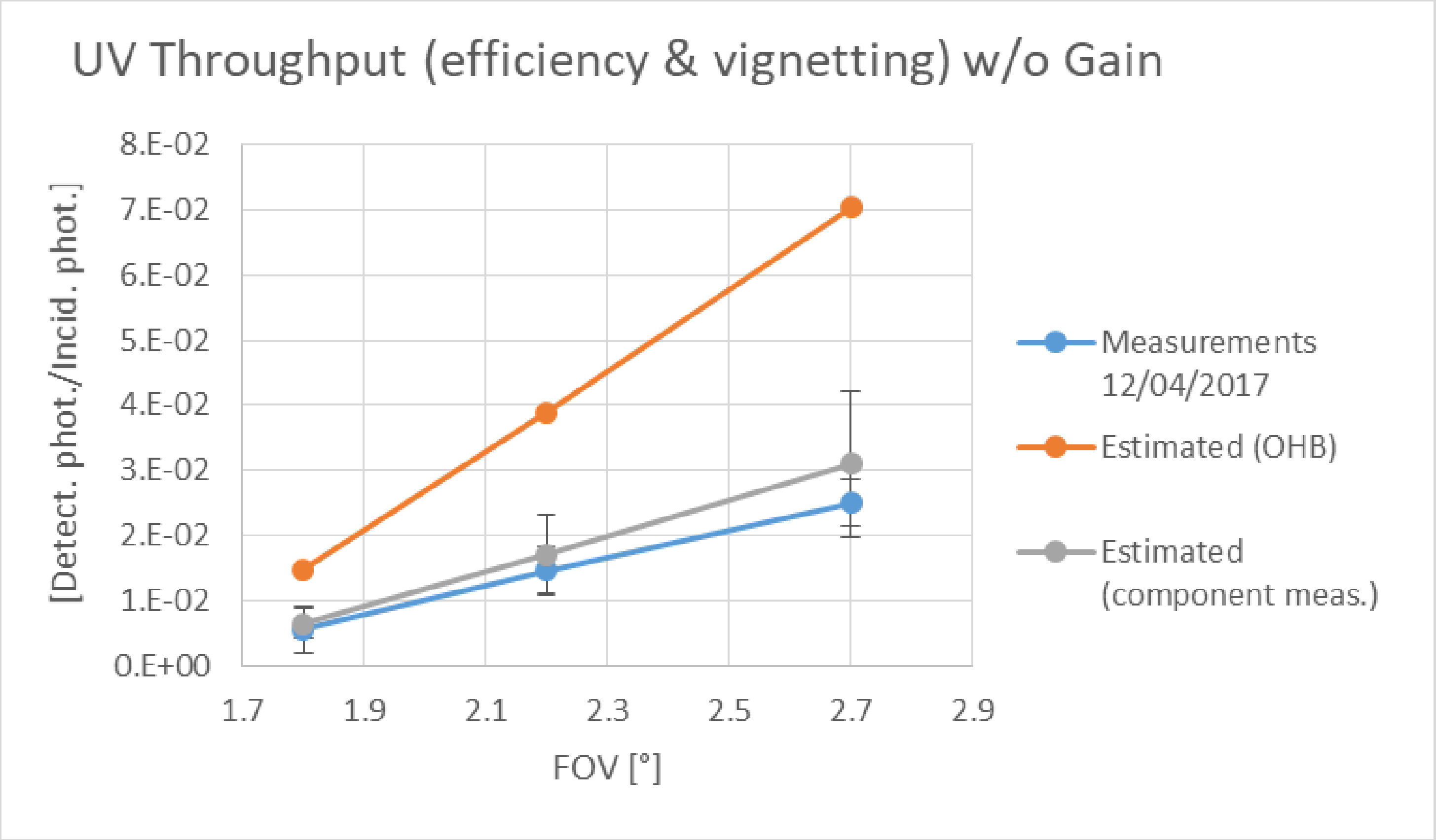

Response Efficiency [DN/phot.In] = (6.6 ± 0.1)e-1 [DN/s/pxl/phot.In]

UV Throughput Measured during Defocus Test

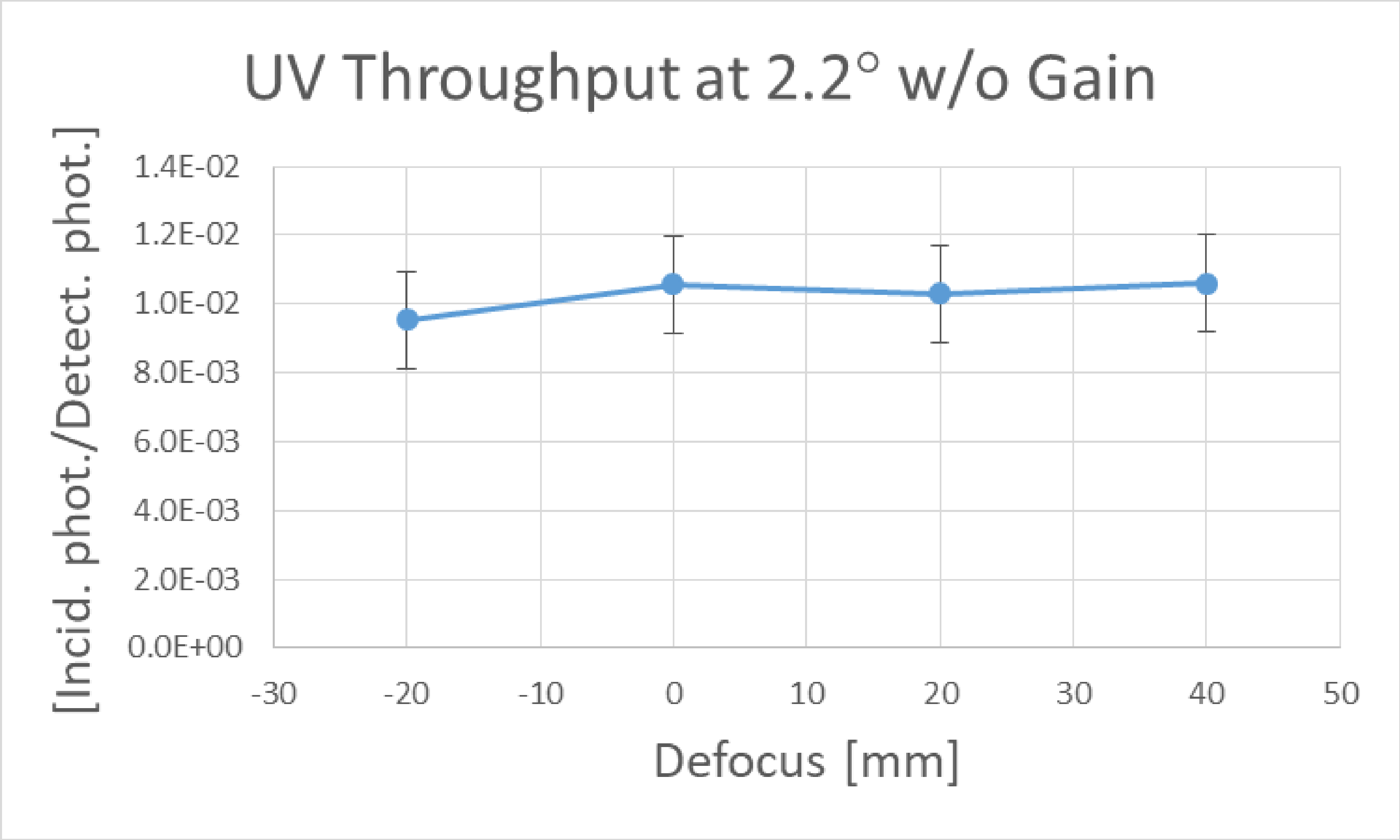

UV Response Efficiency

Response Efficiency = (6.6 ± 0.1)e-1 [DN/s/pxl/phot.In] =

$$= \frac{\text{Response Throughput [DN/s/pxl/phot.In] (measured @ FoV = 1.8°, 2.2 °, 2.7 °)}}{\text{Vignetting@ FoV = 1.8°, 2.2 °, 2.7 ° (derived from VL radiometric calibration)}}$$

VL Polarimeter Calibration

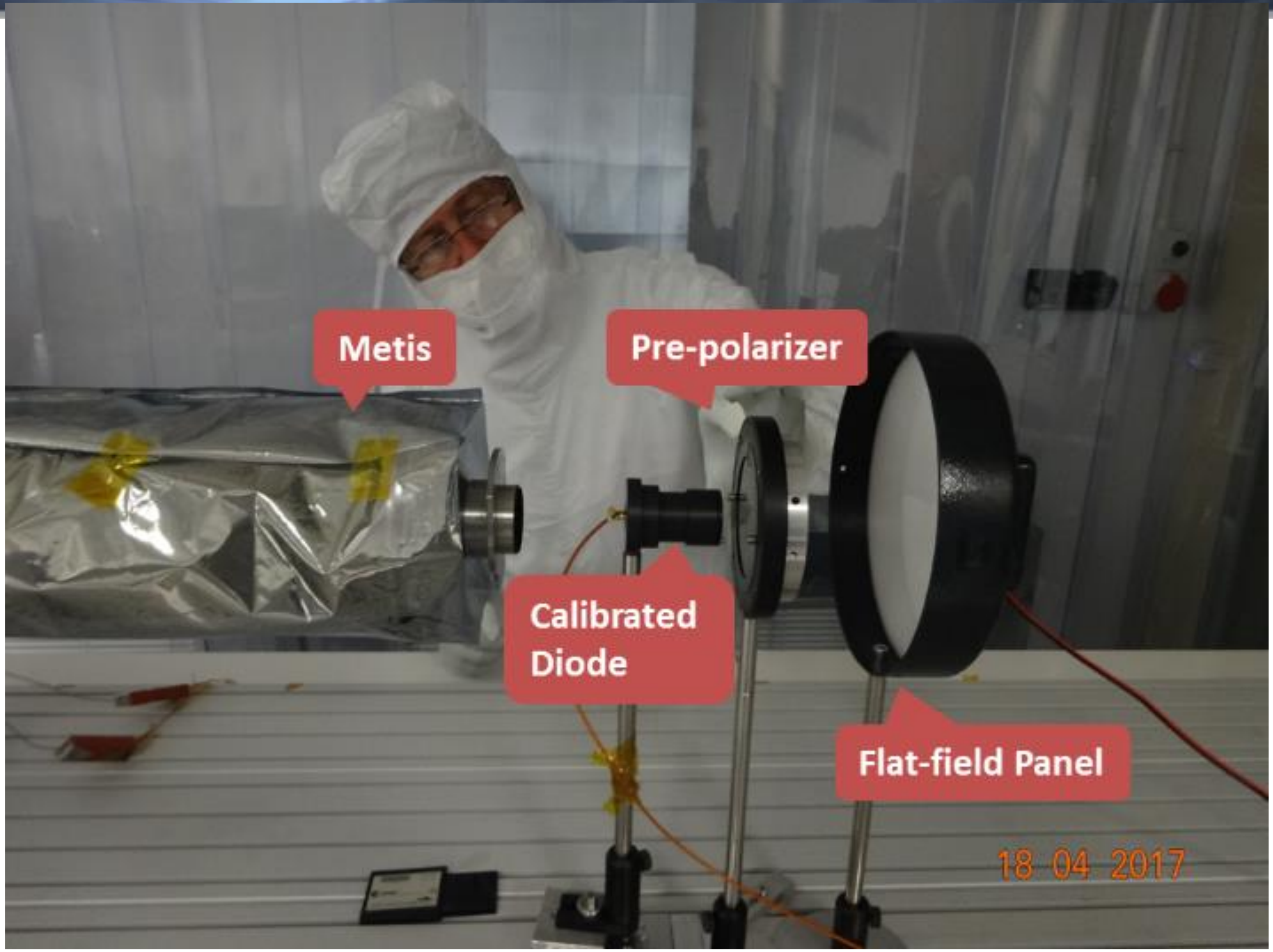

Frames of Reference

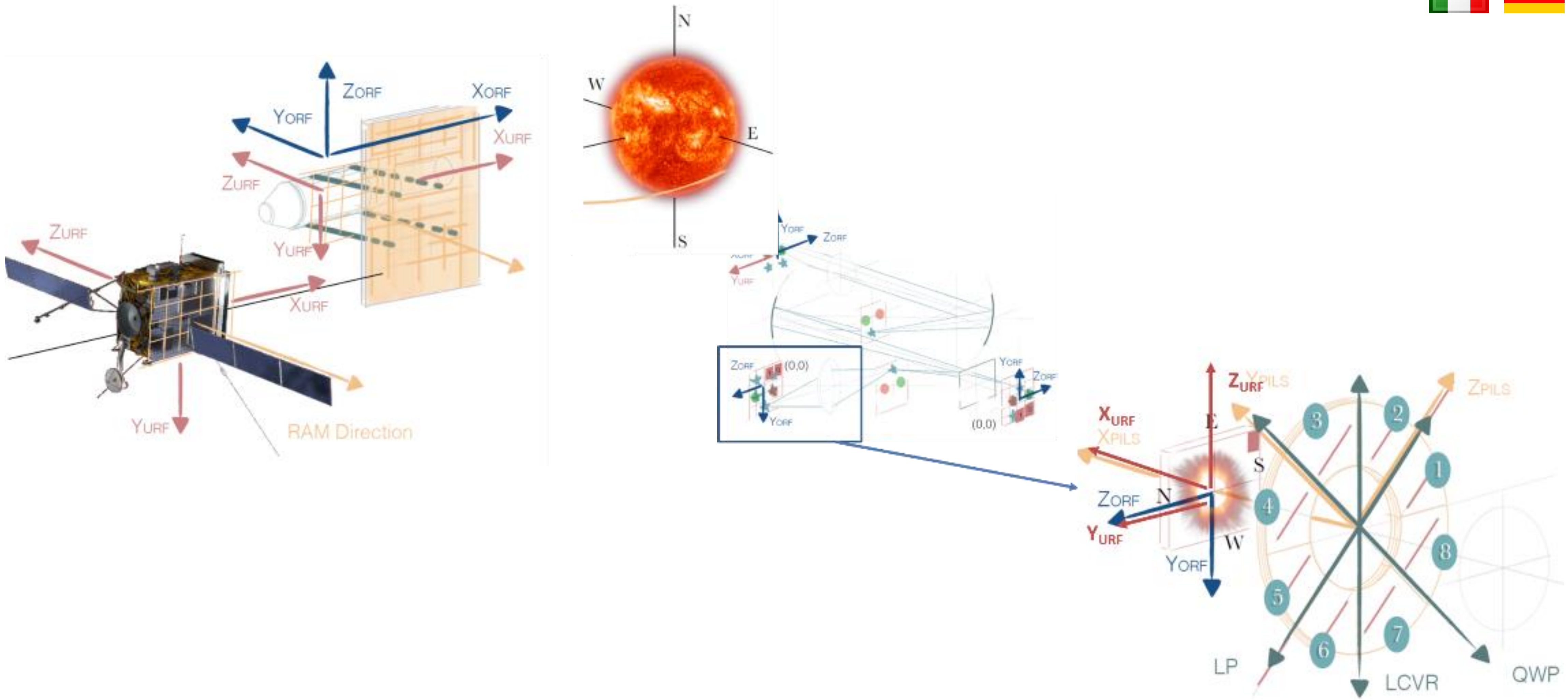

Polarimentry Data Analysis & Results

Experimental Data

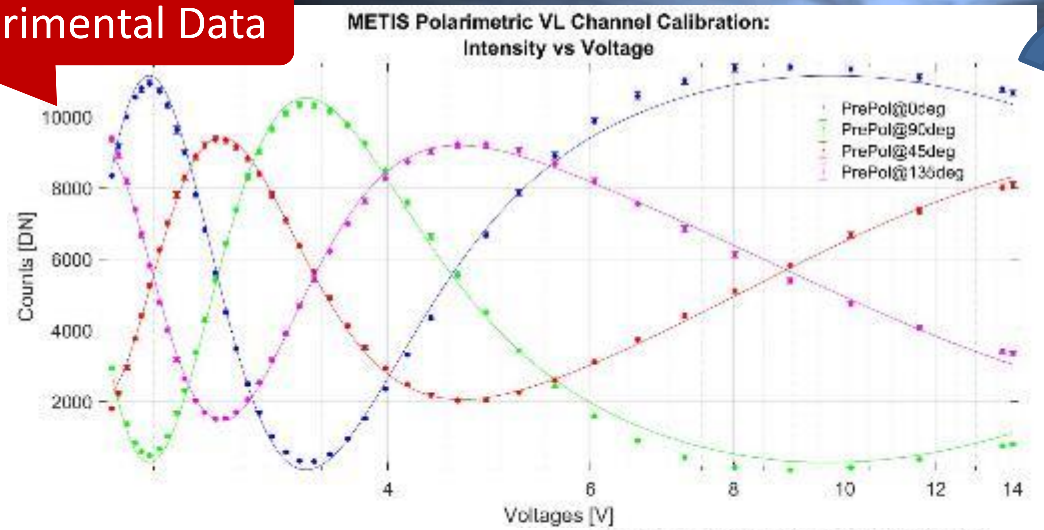

Malus Curve

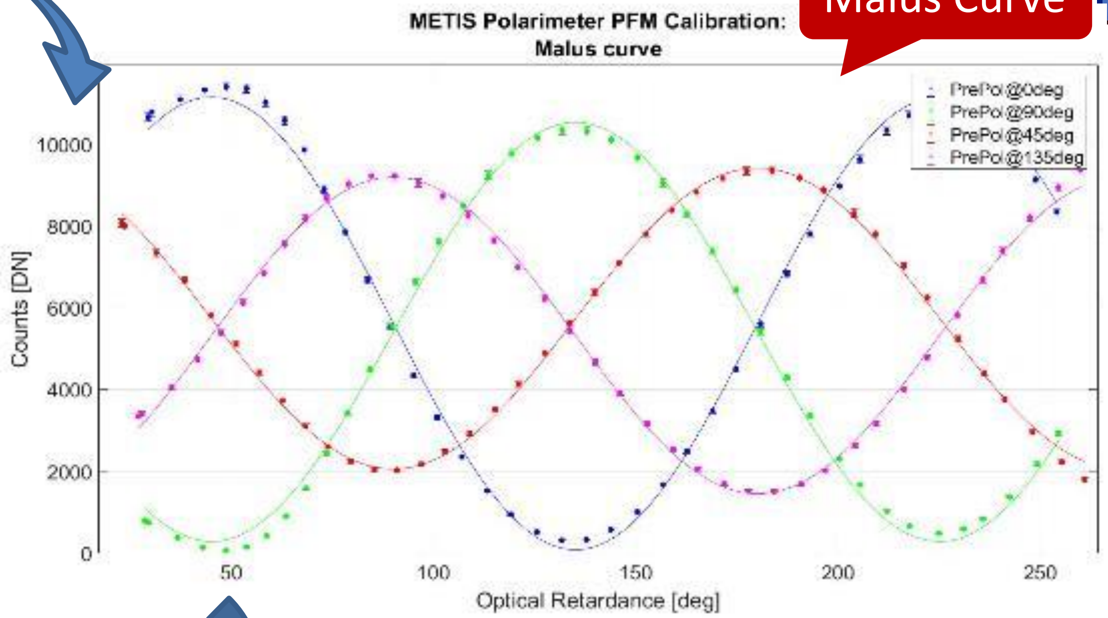

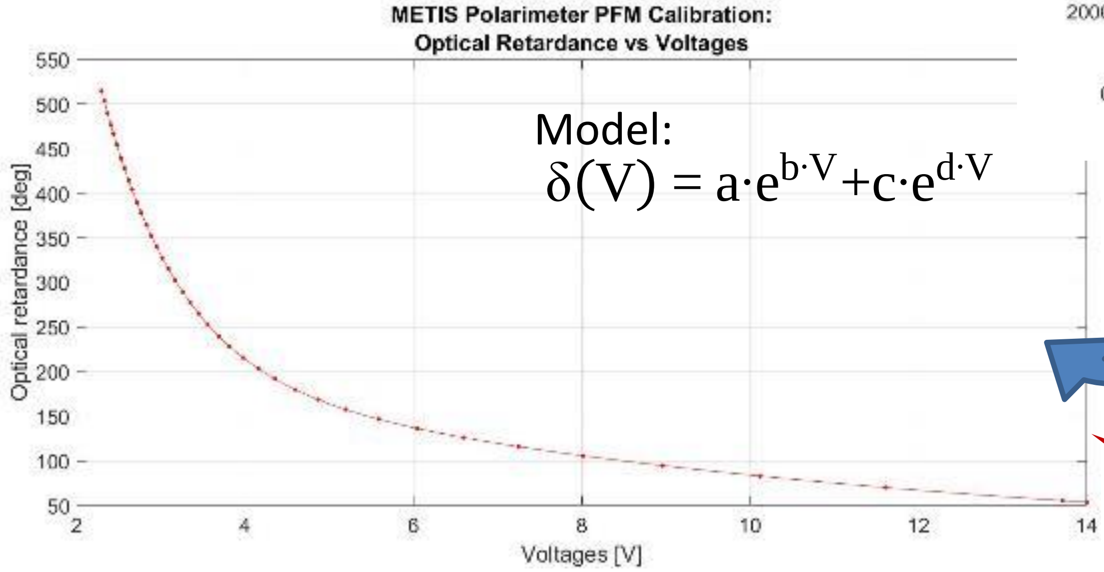

Model:

$$\delta(V) = a \cdot e^{b \cdot V} + c \cdot e^{d \cdot V}$$

Retardance-Voltage Curve

Demodulation Tensor Measurement

The demodulation matrix must be measured, and the accuracy to which it is known will determine the accuracy of the measured Stokes parameters.

The incoming light Stokes parameters are obtained by inversion:

4 x 3

$$\boldsymbol{m} = \boldsymbol{X} \cdot \boldsymbol{S} \quad \Rightarrow \quad \boldsymbol{S} = \boldsymbol{X}^{-1} \cdot \mathbf{m}$$

Inversion Problem!!

Method:

Moore-Penrose pseudoinverse → matrix that can act as a partial replacement for the matrix inverse in cases where it does not exist. This matrix is frequently used to solve a system of linear equations when the system does not have a unique solution or has many solutions.

Demodulation Tensor

Evaluated on the whole image

Demodulation Matrix Element	Theoretical value	Mean of the computed value	Std of the computed values
x^{+}_{11}	0.5	0,50	0,00
x^{+}_{12}	0.5	0,50	0,00
x^{+}_{13}	0.5	0,50	0,00
x^{+}_{14}	0.5	0,50	0,00
x^{+}_{21}	1	1,12	0,15
x^{+}_{22}	0	0,47	0,38
x^{+}_{23}	-1	-1,39	0,25
x^{+}_{24}	0	-0,19	0,24
x^{+}_{31}	0	-0,29	0,20
x^{+}_{32}	1	1,35	0,34
x^{+}_{33}	0	0,06	0,33
x^{+}_{34}	-1	-1,16	0,31

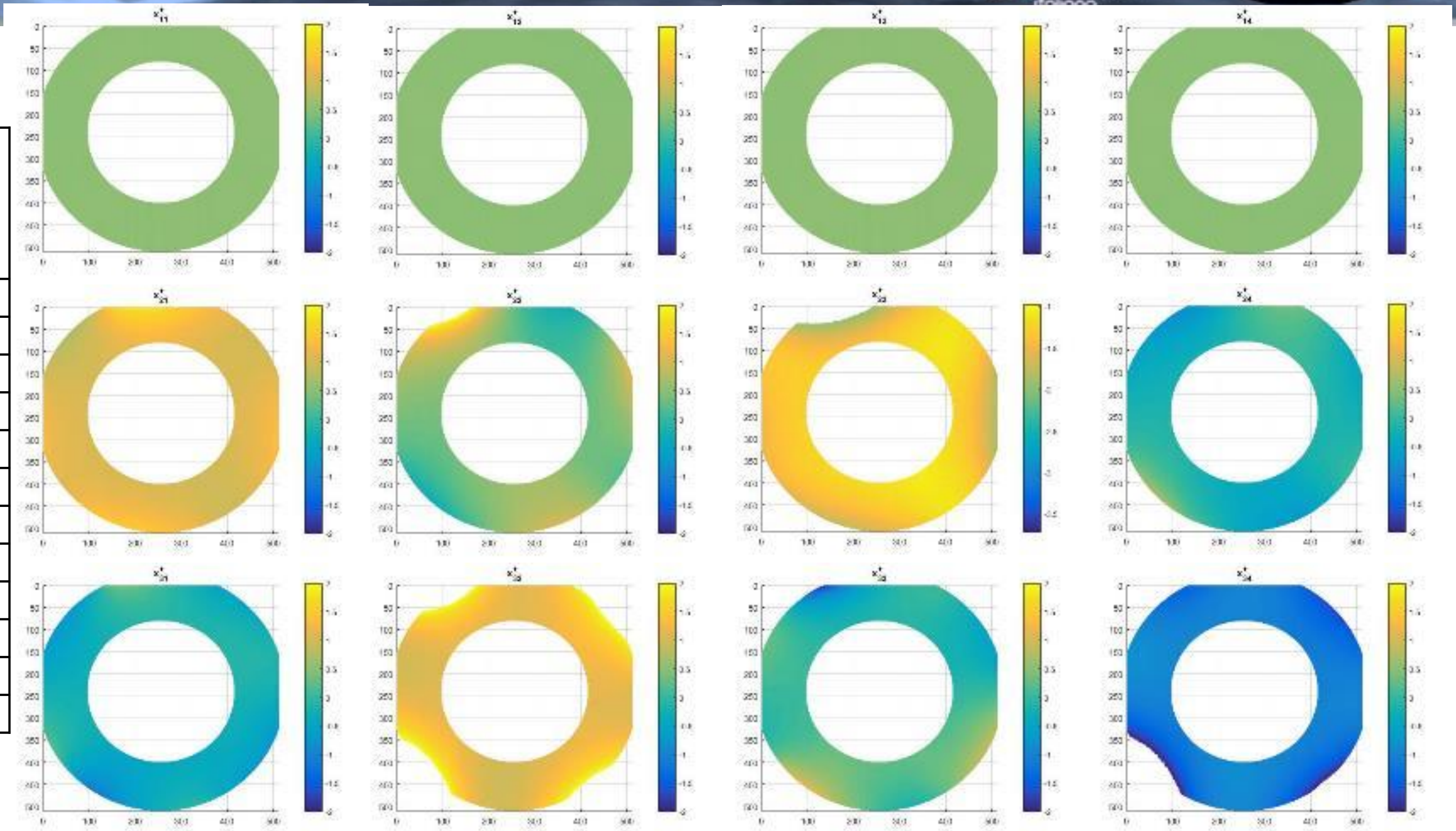

Cfr. VL channel calibration
Session 11b Thursday 15:00
Marta Casti

Demodulation Tensor

$$X^{+} = \frac{1}{2}\begin{pmatrix} 1 & 1 & 1 & 1 \\ 2 & 0 & -2 & 0 \\ 0 & 2 & 0 & -2 \end{pmatrix}$$

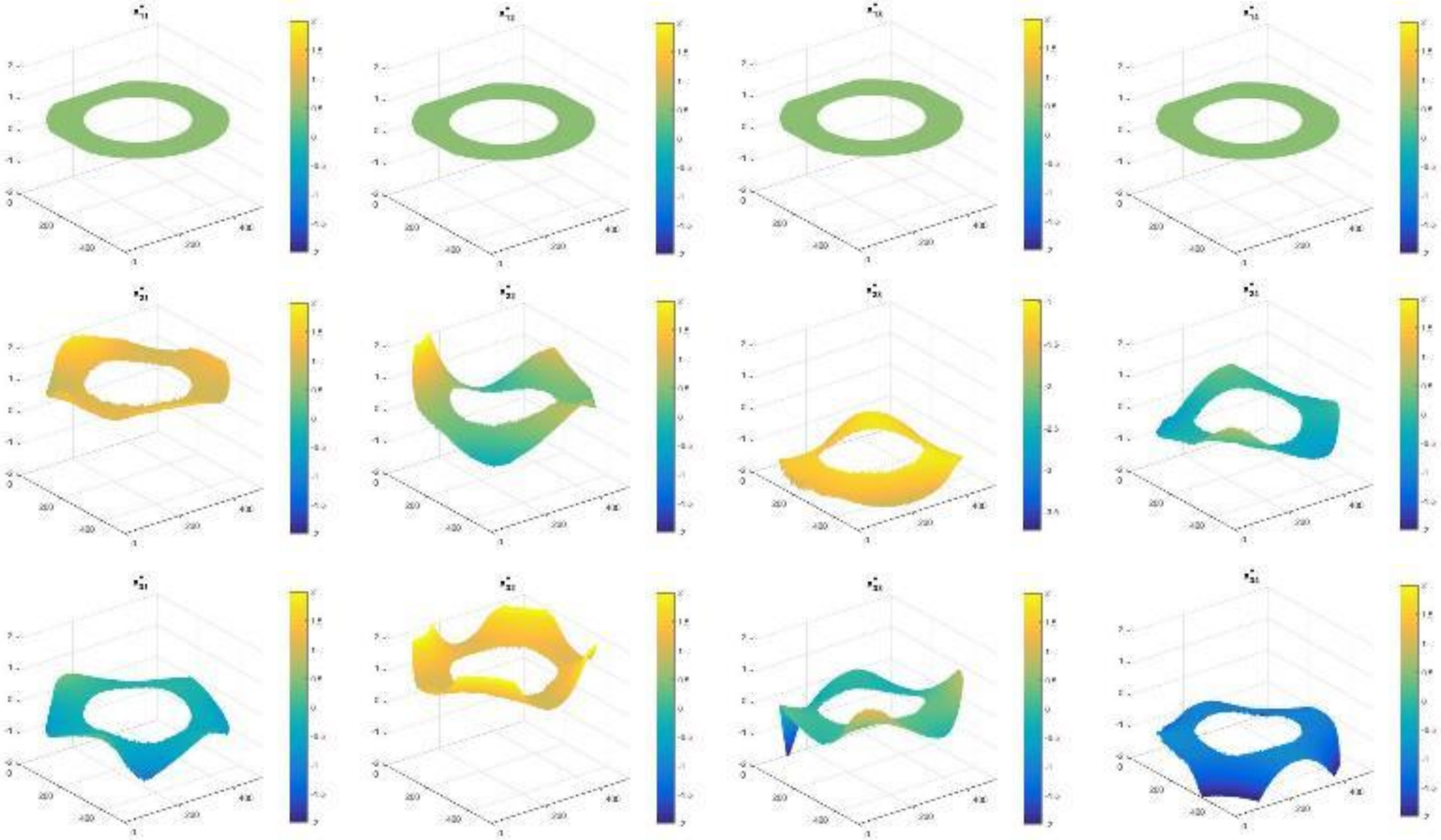

Demodulation Matrix
(parameters varability across the focal plane)

$$X^{+} = \frac{1}{2}\begin{pmatrix} 1 & 1 & 1 & 1 \\ 2 & 0 & -2 & 0 \\ 0 & 2 & 0 & -2 \end{pmatrix}$$

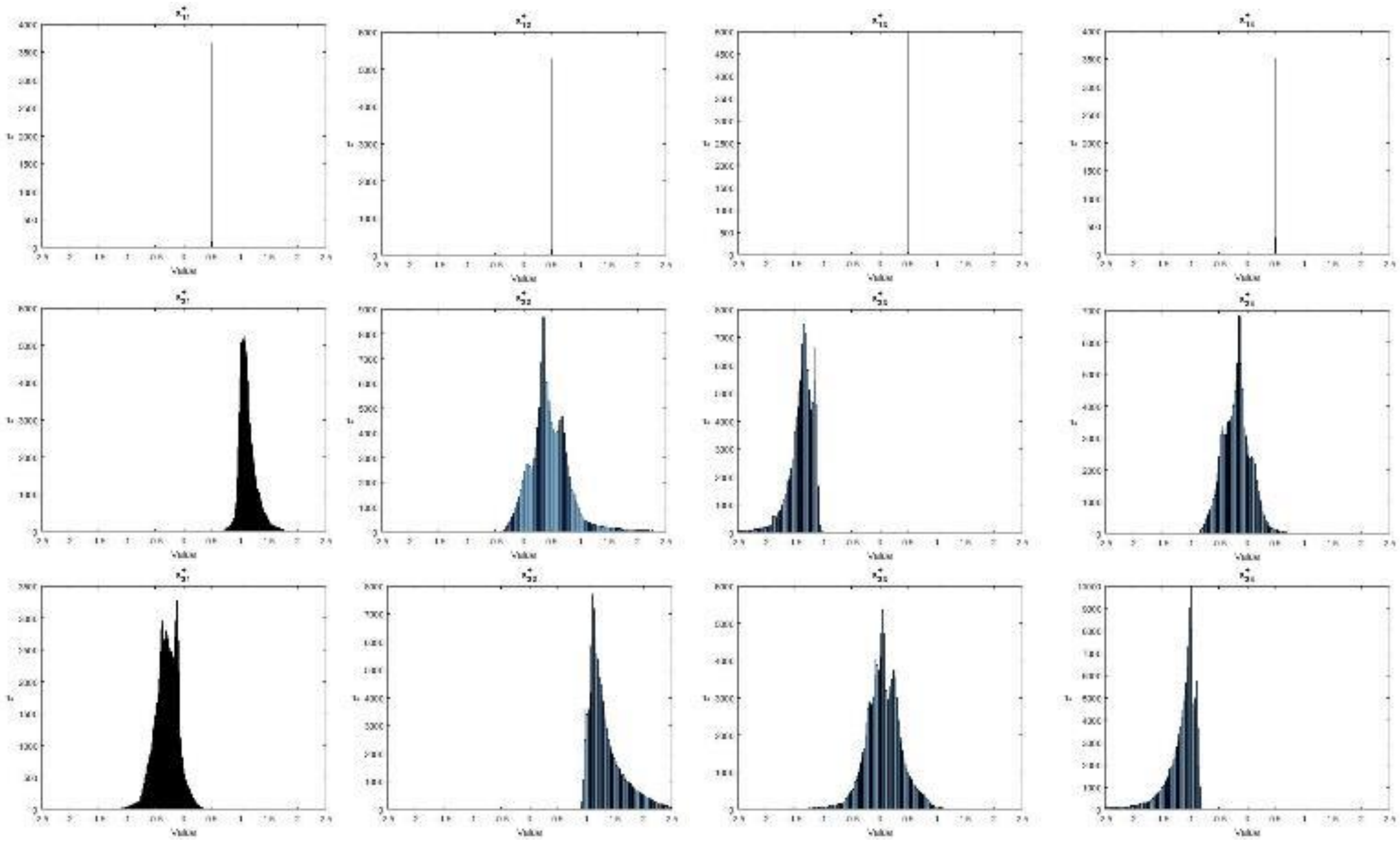

Polarimetry of an Extended Source

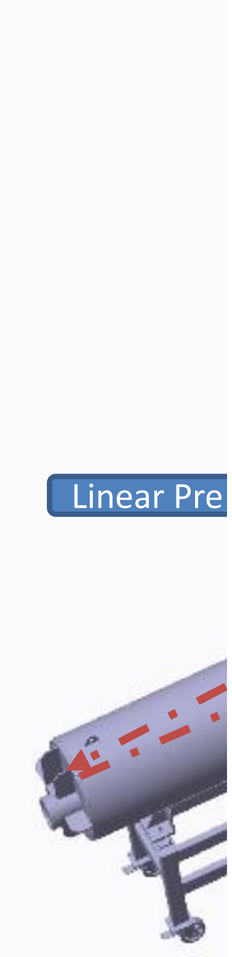

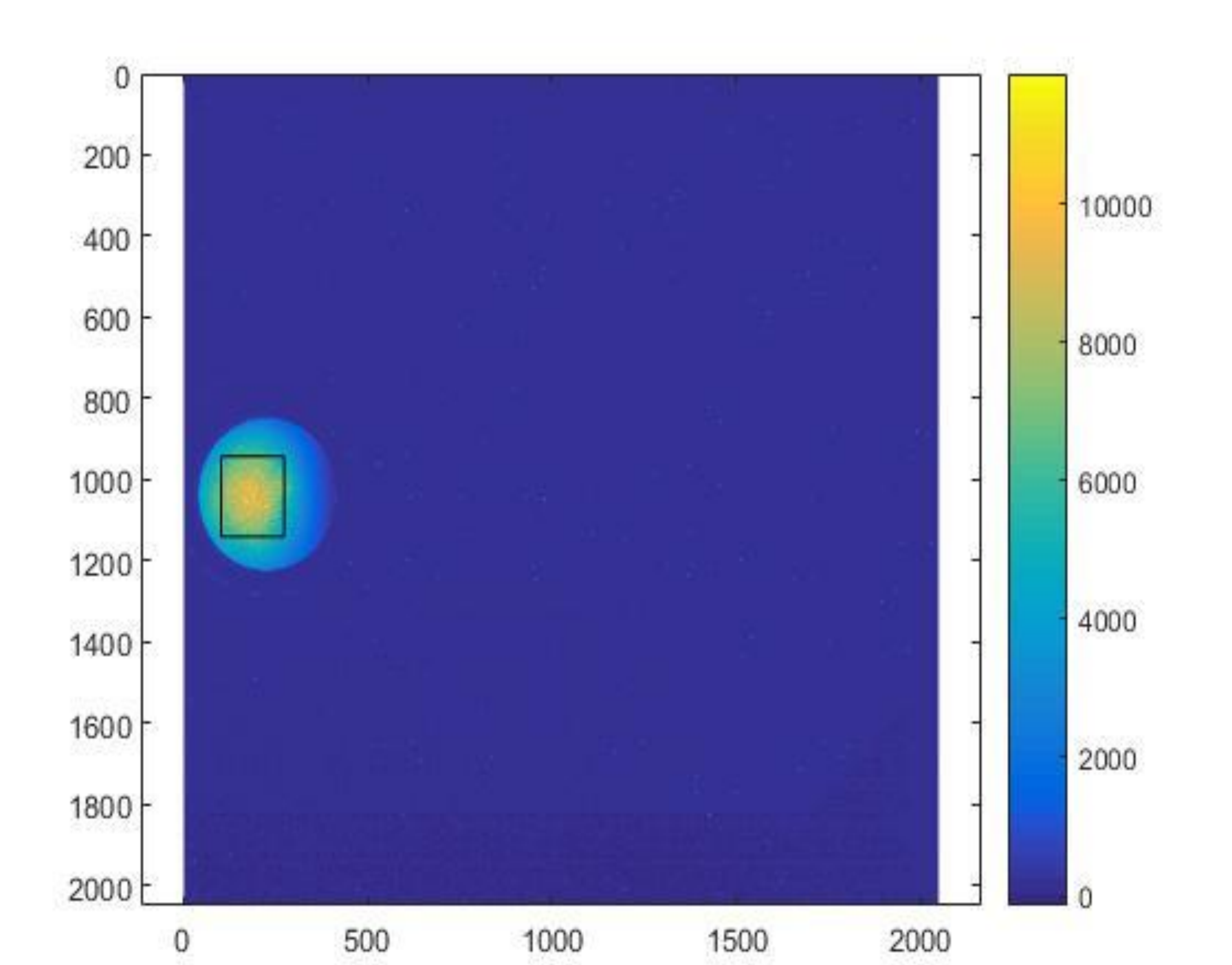

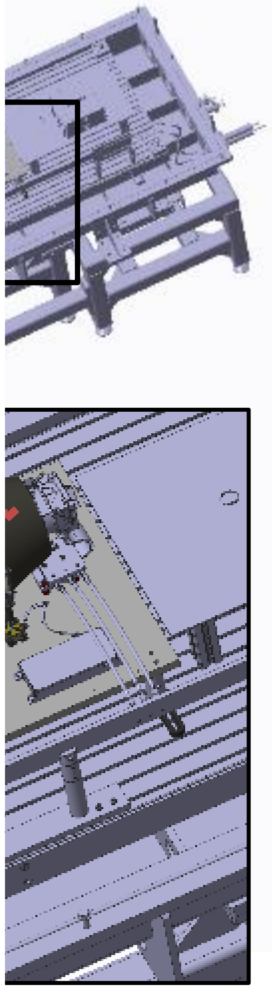

Demodulation Matrix Verification

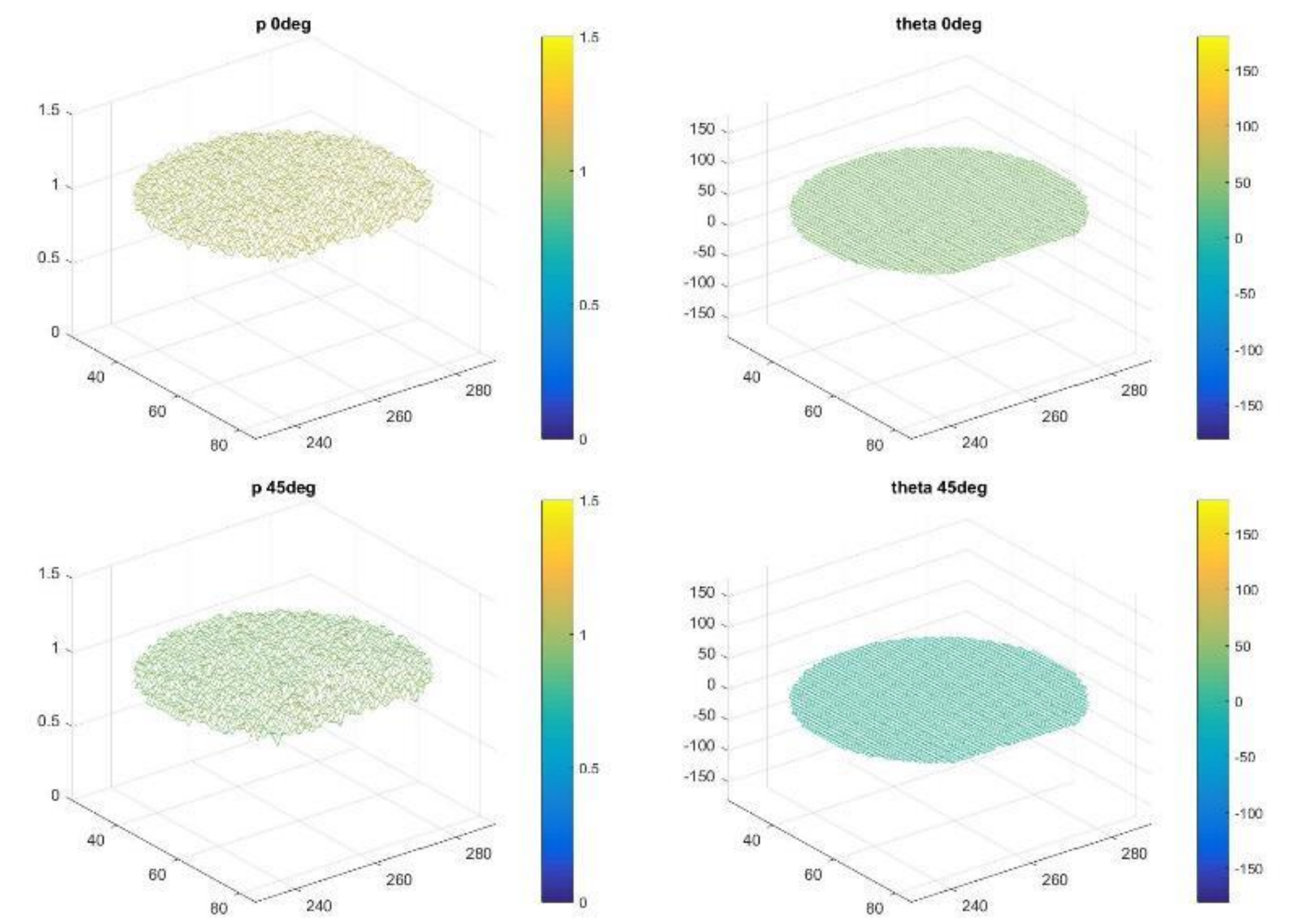

Demodulation Matrix Verification

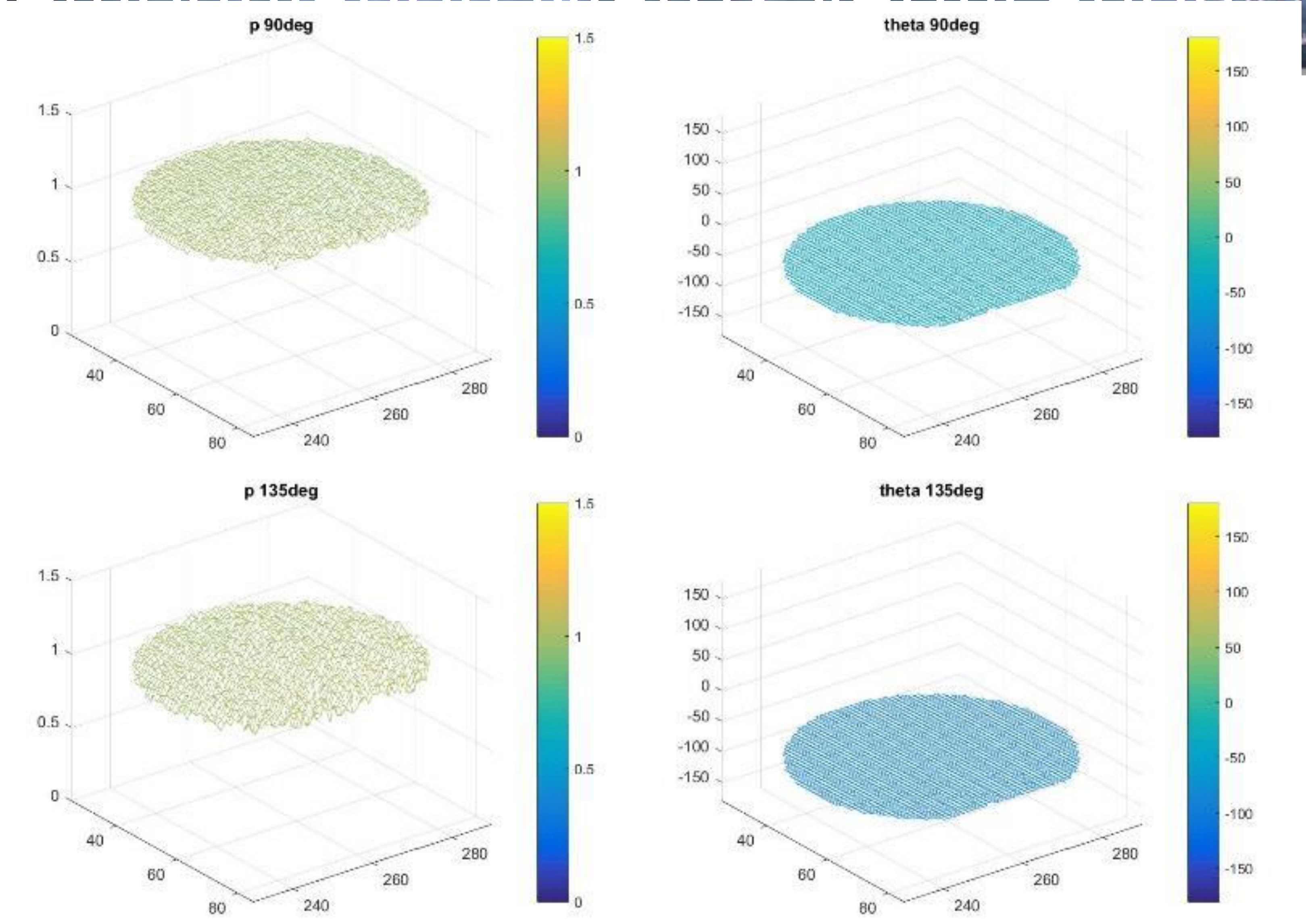

Demodulation Matrix Verification

PrePol Position [deg]	p : Theoretical value	p: Mean of the computed value	p: Standard deviation of the computed value	θ : Theoretical value [deg]	θ: Mean of the computed value [deg]	θ: Standard deviation of the computed value [deg]
0	1	1,04	0,02	45	43,29	0,42 (~ 0,01 rad)
45	1	0,94	0,02	0	-1,04	0,36 (~ 0,01 rad)
90	1	0,99	0,01	-45	-44,01	0,39 (~ 0,01 rad)
135	1	1,00	0,02	90	89,68	0,27 (~ 0,01 rad)

$$\sigma_{th}(p) = \frac{1}{SNR} = \sqrt{\frac{G}{DN}}$$

$$\sigma_{th}(\theta) = \frac{\sigma_{th}(p)}{p}$$

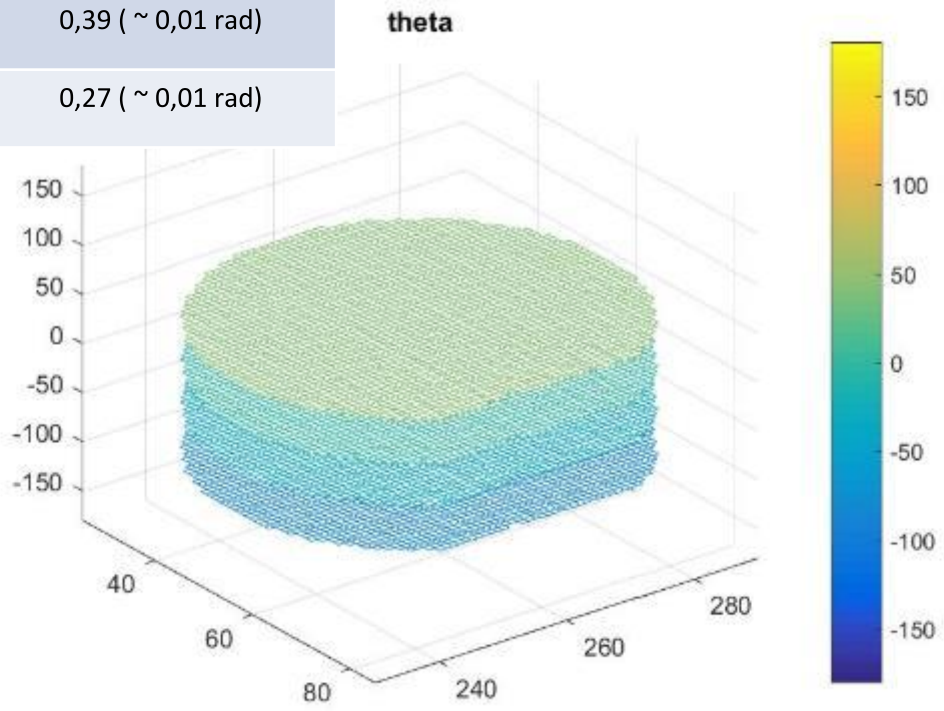

SPOCC Set-up for Stray-Light Measurements

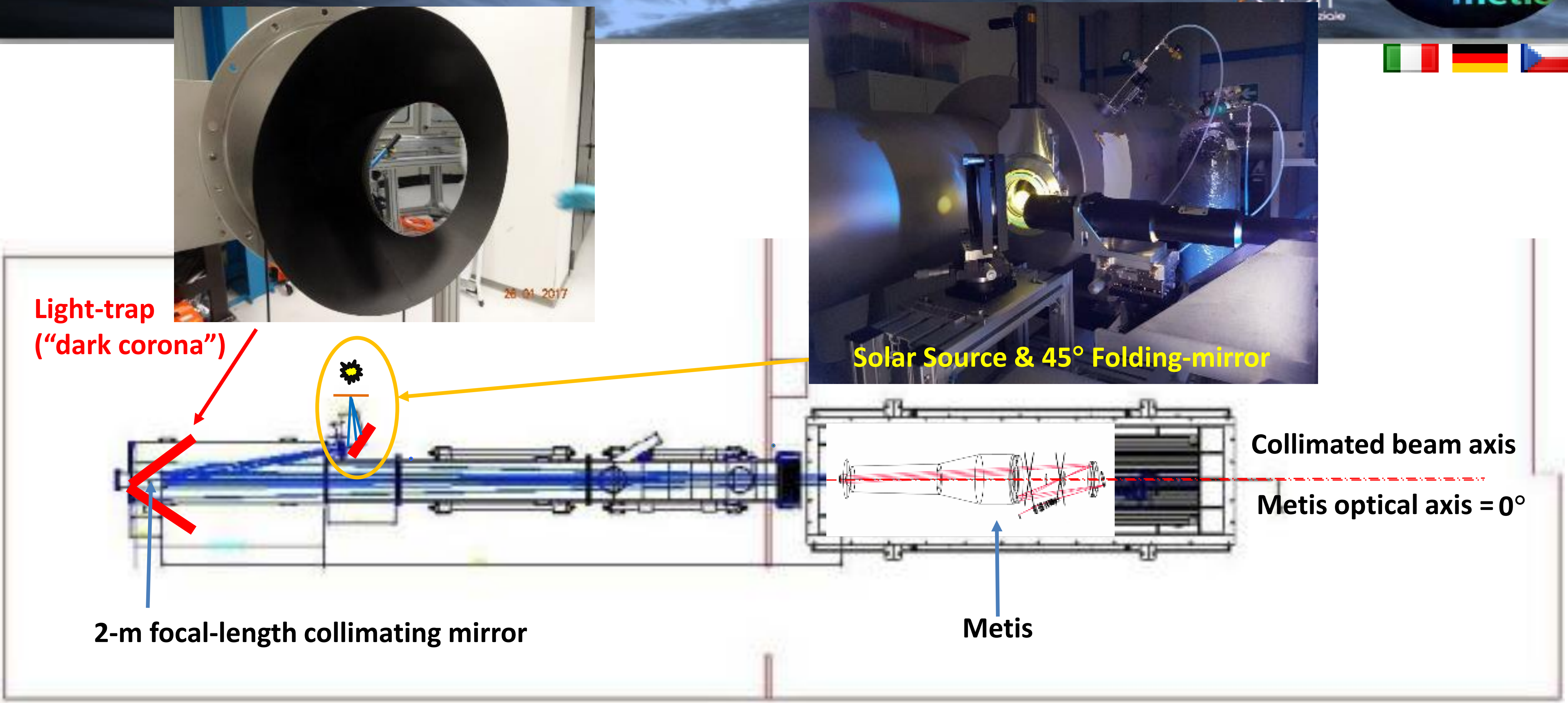

SPOCC Light-trap

Required level of suppression of the stray-light: $B_{stray} / B_{Sun} \leq 1.e\text{-}9)$

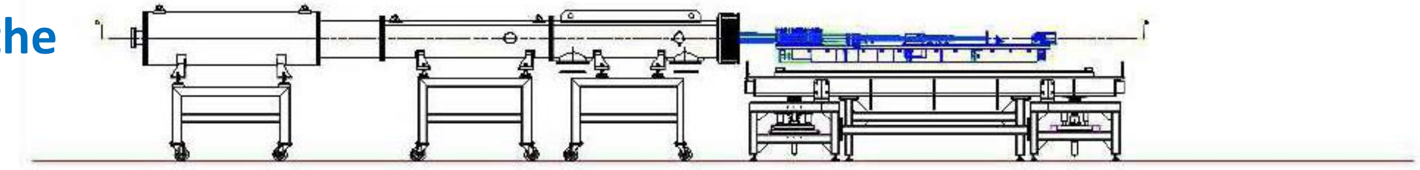

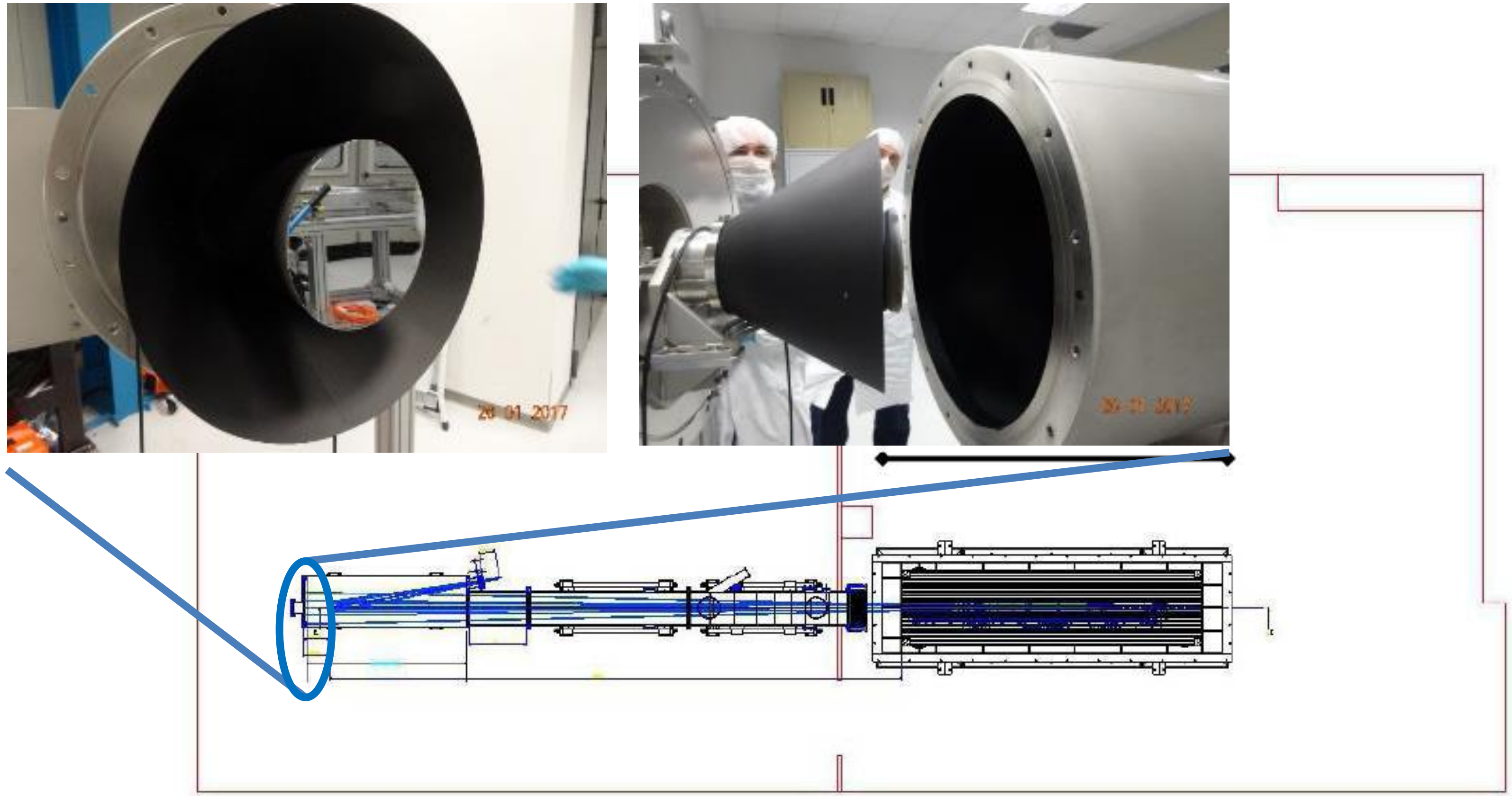

SOCC Pipeline Baffling

- The bright halo was mainly due to a back reflection of one of the first baffle in the pipeline blackened only by Aeroglaze.

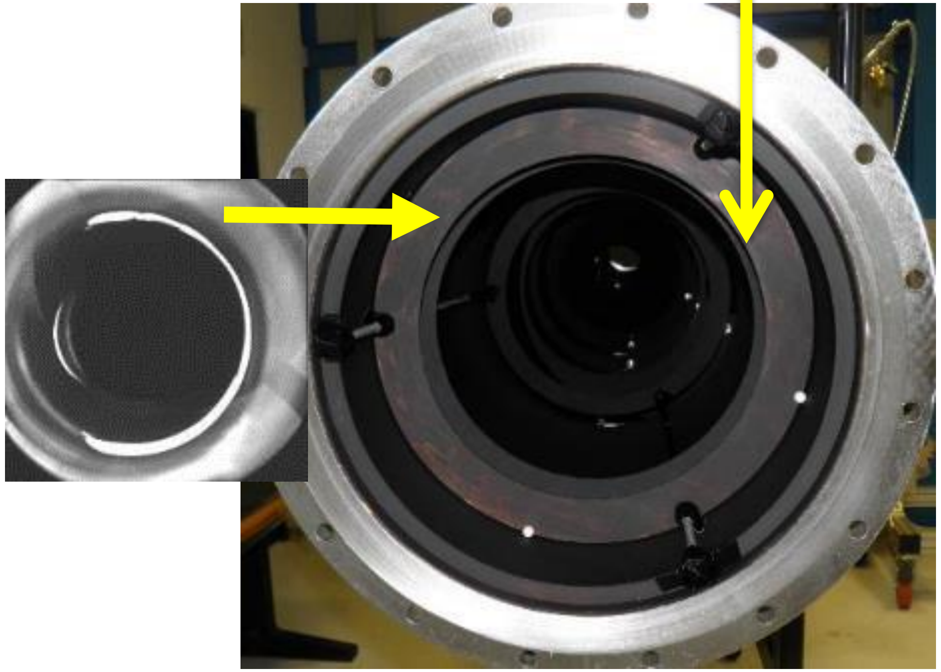

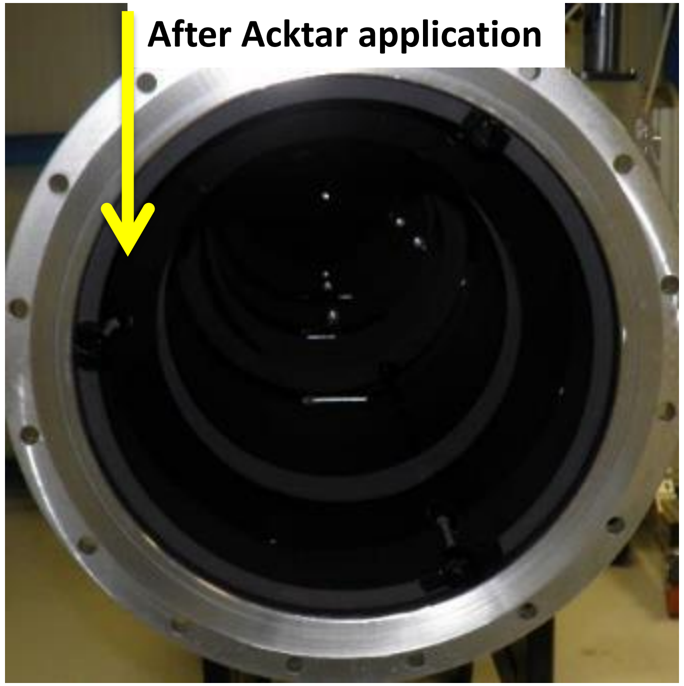

Stray light at 0.5 AU before IO position fine tuning

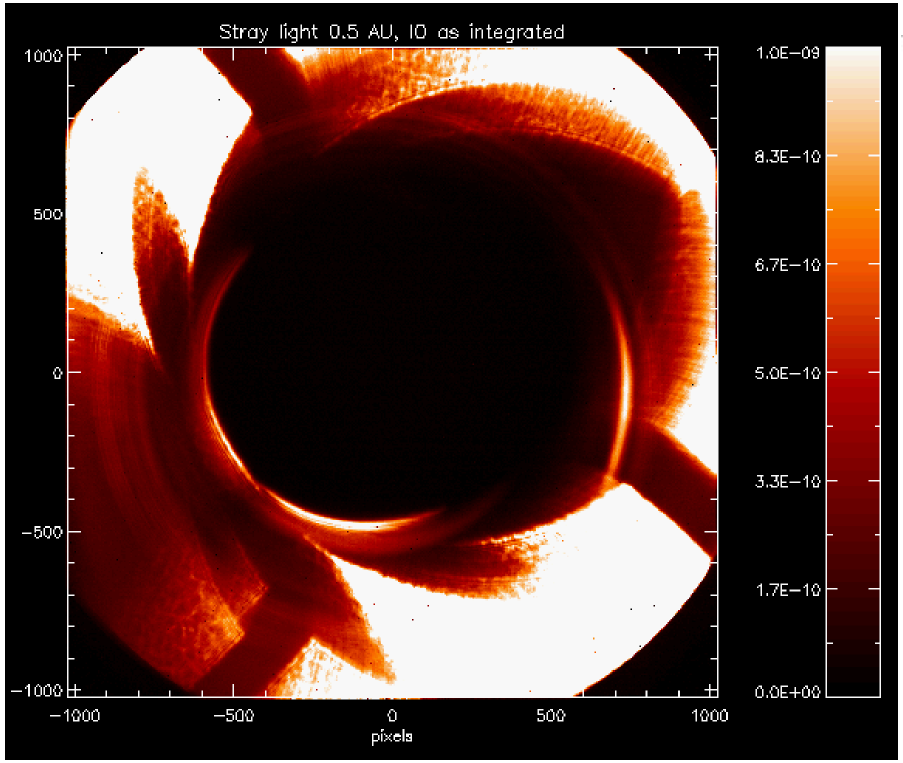

Acquired image

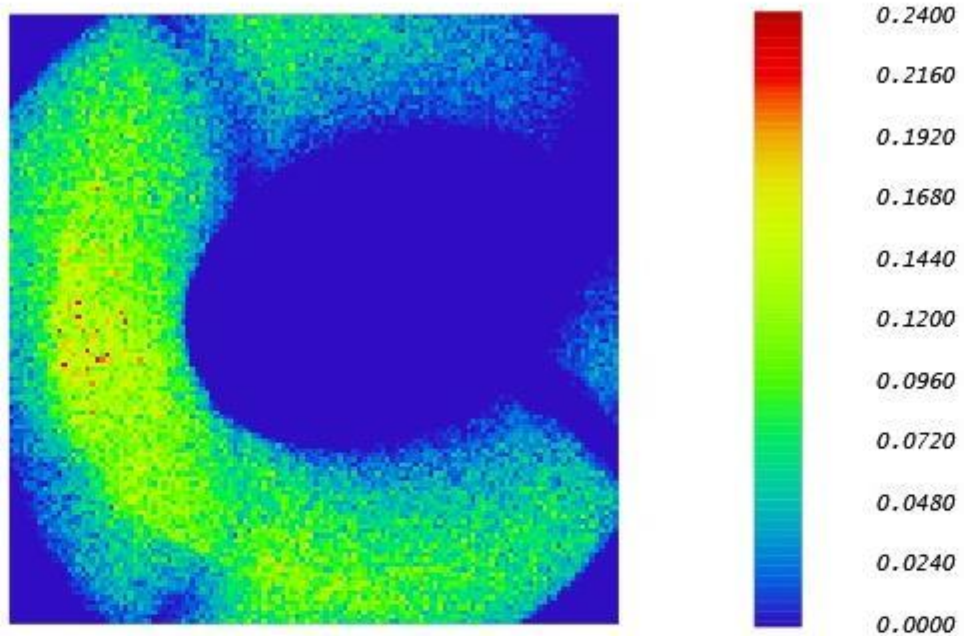

Zemax simulation with off-centered IO

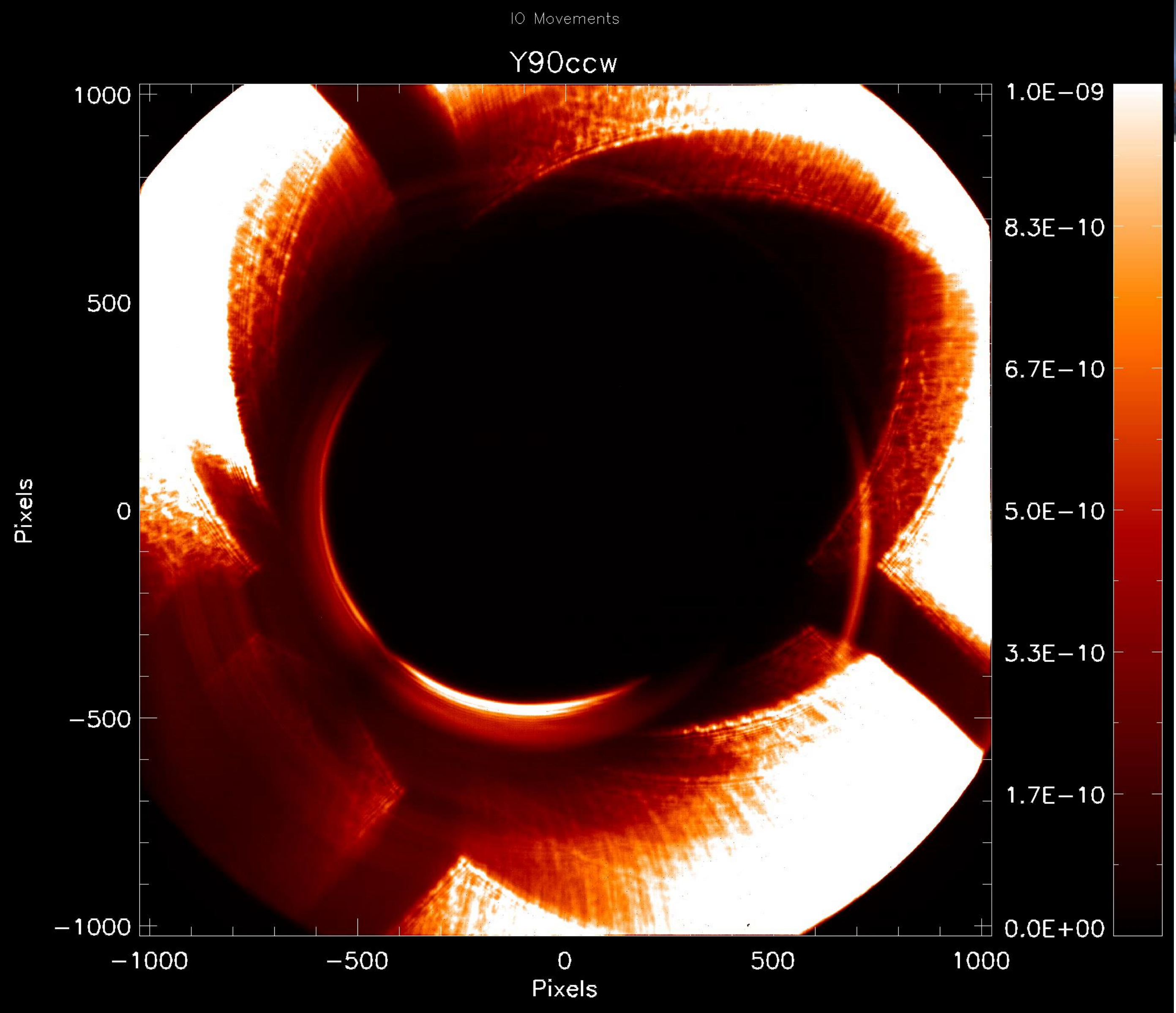
IO Movements
Y90ccw
1000
500
0
−500
−1000
Pixels
−1000
−500
0
500
1000
Pixels
1.0E−09
8.3E−10
6.7E−10
5.0E−10
3.3E−10
1.7E−10
0.0E+00

Stray light at 0.5 AU

Level of suppression of the stray-light from the Sun at 0.5 A.U. (“dark corona”):

$B_{stray} / B_{Sun} \leq 5.e\text{-}10$

(Req.: $B_{stray} / B_{Sun} \leq 1.e\text{-}9$)

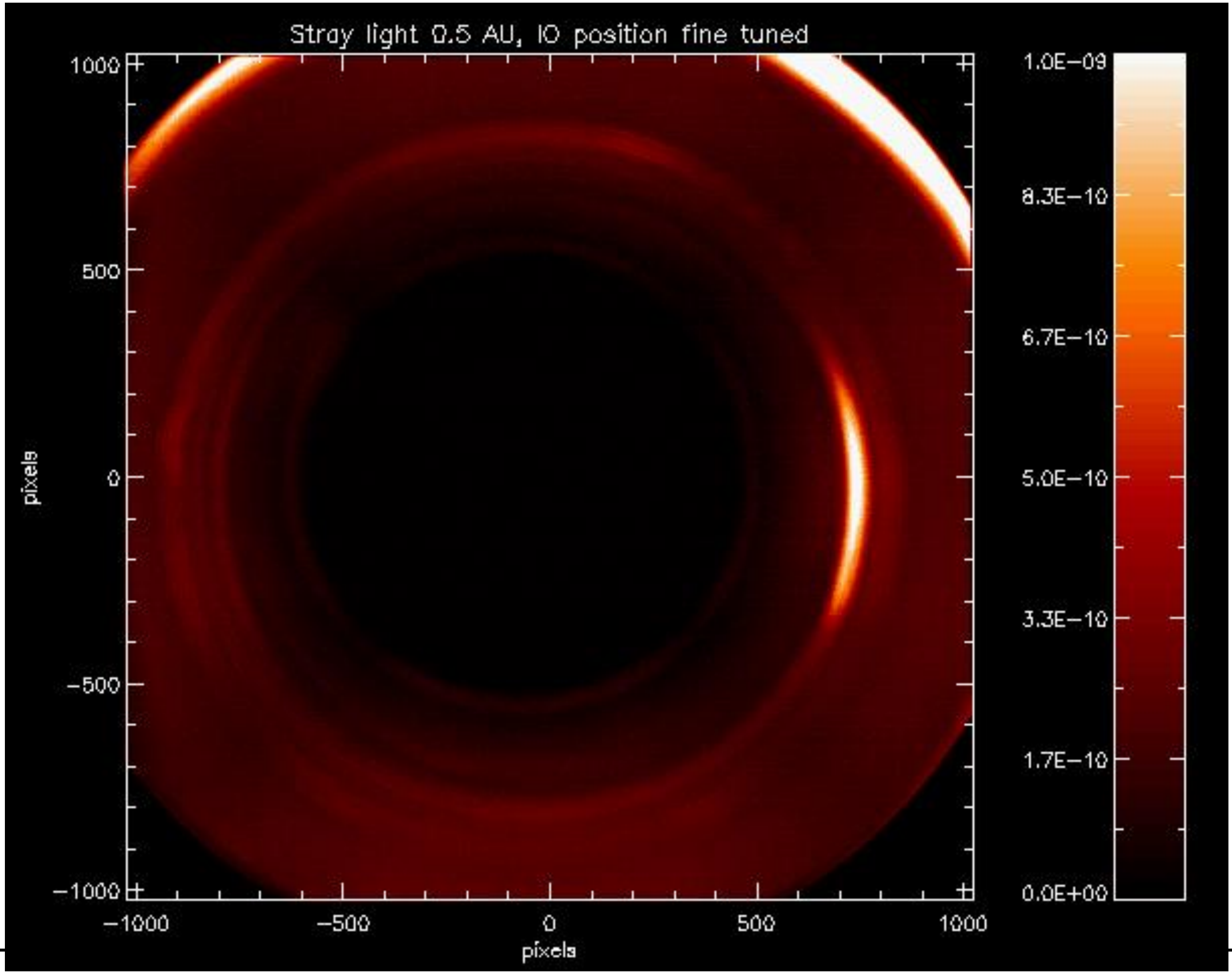

Conclusions

- Vignetting function (Flat-Field) ✓ according to ray-trace
- VLDA Photon Transfer Curve ✓ matching component-level calibration
- VL Imaging & Radiometric Performance ✓ within specs
- UV Imaging ✓ PSF > × 3 wrt ray-trace (VL-UV alignment balancing)
- UV Radiometric Performance ✓ less then a factor 2.3 wrt estimated (due to mirror coating: 54% vs expected 80%)
- VL Polarimeter Performance ✓ within specs
- Stray-light Suppression Performance ✓ within specs

S. Fineschi [a],

G. Massone [a], G. Capobianco [a], M.Casti*[a], Landini[b], V. Da Deppo[c], F. Frassetto[d], M. Romoli[e], E. Antonucci [a], V. Andretta[f], G. Naletto[g], G. Nicolini[a], P. Nicolosi[g], F. M. Pancrazzi[e], D. Spadaro[h], R. Susino [a], L. Teriaca[i], M. Uslenghi[l] , M. Castronuovo[m]

- [a] INAF – Osservatorio Astrofisico di Torino, Strada Osservatorio 20, 10025 Pino Torinese, Italy;
- [b] INAF – Osservatorio Astrofisico di Arcetri, Largo E. Fermi 5;
- [c] CNR - IFN, via Trasea 7, 35131 Padova, Italy, 50125 Firenze, Italy;
- [d] Dipartimento di Ingegneria dell'Informazione, Università di Padova, Via Gradenigo, 6/B, 35131 Padova; Italy;
- [e] Dipartimento di Fisica e Astronomia – Università degli Studi di Firenze, Via Sansone 1, Sesto Fiorentino, Italy;
- [f] INAF - Osservatorio Astronomico di Capodimonte, Salita Moiariello, 16, 80131, Napoli, Italy;
- [g] Dipartmento di Fisica e Astronomia "Galileo Galilei" - Università di Padova,Via Marzolo, 8 I-35131 Padova, Italy;
- [h] INAF - Osservatorio Astrofisico di Catania, Via S. Sofia 78, 95123 Catania, Italy;
- [i] Max Planck Institute for Solar System Research, Justus-von-Liebig-Weg 3, 37077 Göttingen, Germany;
- [l] INAF - IASF, Via E. Bassini 15, 20133, Milano, Italy
- [m] ASI, Via del Politecnico 00133 Roma, Italy